

Analysis of voltage control using V2G technology to support low voltage distribution networks.

Marina Mattos¹, Joao Archetti², Leonardo Bitencourt², Alexander Wallberg¹, Valeria Castellucci¹, Bruno Dias², and Janaína G. Oliveira³

¹Uppsala Universitet

²Universidade Federal de Juiz de Fora

³Uppsala University Faculty of Science and Technology

June 6, 2023

Abstract

The decarbonization of the power generation and transport sector encourage the analysis of connection of DER, such as EVs, to the electrical system, as well as the evaluation of their impact on smart cities. A better understanding of the negative impacts on the power systems will lead to propose mitigation measures and eventually revolutionize the way distributed generation works. This paper aims at modeling and evaluating the impact of EVs on a real distribution network. The energy system chosen operates at 60 Hz, 34,5 kV (Medium Voltage) and 0,208 kV (Low Voltage) and it is simulated using PSCAD/EMTDC. To reproduce realistic user consumption profiles, dynamic load profiles based on EV owners behaviour have been simulated. The V2G technology is modeled to mitigate the impacts of high penetration of EVs by supporting the network from undervoltage. The results show the importance of active management in modern power systems, especially considering the increase in DER penetration expected for the coming years. This work shows the benefits of implementing V2G technology while highlighting the challenges involved in a real case.

Introduction

Government policies have been developed in several countries aimed at decarbonizing the power generation and transport sector. The 2030 Agenda is a global action plan created by the UN which brings together 17 SDG and 169 goals signed by 193 Member States. Clean and affordable energy SDG 7 and sustainable cities and communities SDG 11 have been the focus of current governments as a way to meet the commitment by 2030 through conscientious, sustainable, efficient and reliable development ([ONU, Access: 07 December, 2022](#)).

The EVI is a multigovernmental policy aimed at encouraging and accelerating the adoption of electromobility. It was created in 2010 within the framework of Clean Energy Ministerial. EVI is a platform to share knowledge among member countries, with a biannual meeting aiming at overcoming political and governmental challenges related to the adoption of EVs ([IEA, Access: 08 December, 2022](#)). The IEA acts as a coordinator to support member governments of the EVI.

Recently, the members of the European Parliament voted in favor of banning the sale of diesel and gasoline cars from 2035 onwards to reduce greenhouse gases and decrease dependence on fossil fuels. It is worth mentioning that for the mass adoption of EV regulations and deployment of charging infrastructure, especially in urban areas are necessary.

Considering the associated incentives, it becomes strategic to analyze the implementation and connection of DER, such as EVs into the electrical system, as well as evaluating their impacts. The capacity to host EVs depends on many aspects of the network. More robust energy systems, such as Uppsala and Stockholm in Sweden, allow a considerable amount of electric vehicles be connected without significant impacts on the network, such as undervoltage or transformer overload. On the other hand, there are more sensitive networks that need to be studied regarding the analysis of EVs penetration and V2G control, such as countries in Latin America. Understanding these impacts is essential to propose mitigation and suggest modifications in regulations of distributed generation (ANEEL, June, 2021).

The work presented in this paper provides research on a real-world example of V2G. The V2G technology involves bringing available energy from the car into the smart grid. Benefits include facilitating ancillary services, reducing costs and conscious and sustainable development. Network expansion is expensive, hence, using existing resources more effectively is the focus of current research, for example, the collaboration between the UU, a foundation for cooperation between the universities in Uppsala, business, and society – called STUNS and UPAB operating a parking garage at Dansmästaren, also known as mobility house. The Dansmästaren is a test bed where different DER are implemented as a research opportunity to contribute as a smart building and Uppsala as a more sustainable city (Flygare et al., 2022) (Castellucci et al., 2022). The goal is to use the test bed to understand the V2G control implement in the parking garage in the future.

The proposed V2G Control is based on using stationary EV as an energy reserve for the electrical network, the control is carried out in a way that is economically attractive for the user, encouraging the vehicles owner to supply the network through ancillary services. When the electricity tariff is high (peak hours) the EV could supply the network, providing energy and acting as a mitigating element. When the fare is low, the EV battery is charged and the vehicle acts as a load. For V2G to work, it is necessary to develop a smart grid, capable of having equipment with bidirectional communication and real-time measurement techniques (de Arruda Bitencourt, 2018).

The present work focuses on V2G control technology, and its analysis has been implemented in a power system model based on a real network (Singirikonda et al., 2022) (Nasr Esfahani et al., 2022). There are several challenges related to V2G that prevent it from reaching its application potential, being an essential technology for the development of smart grids (Han & Xiao, 2016). To properly study and assess the impacts related to congestion of assets and voltage levels, it is essential to thoroughly study real distribution networks with medium and low voltage levels, considering capturing the interactions between the different voltage levels and the phases involved (Zhu et al., 2022).

In the literature, the MEA Project carried out in the United Kingdom, is a pioneer in the implementation of realistic studies of widespread EVs adoption. It is a reference for evaluating the challenges and recurring benefits of mass EVs implementation on the network. The project focused on realistic modeling of EVs analyzing the impacts on the grid, focusing not only on the technical aspects but also on the social aspects, contributing to a better understanding of EVs user behavior (Quirós-Tortós et al., 2018)(Quirós-Tortós et al., 2018).

In line with this, the dissertation (Lazari, 2020) aims to analyze the insertion of EVs in the IEEE 13 buses system. The main focus is to assess the performance of the V2G and V2H control, comparing two different tariffs: the conventional tariff and the white tariff. Another study found in the literature focuses on the connection of PV to charge the EVs batteries with stations located in commercial buildings using V2G (Mouli et al., 2019). Thus, photovoltaic energy charges vehicles using dynamic grid tariffs by scheduling the energy exchange with the grid (V2G), while considering the energy restrictions of the distribution grid to avoid overload.

With regard to field work, the Vehicle-to-Coffee project allowed The Mobility House office to have part of its electricity supply coming from a Nissan Leaf. Based on this project, an innovative pilot project emerged, through a partnership between The Mobility House, ENERVIE, Nissan and Amprion (V2GHub, Access: 7 February, 2023). The project studies the integration of V2G technology into the grid using intelligent

charging and energy management. Thus, for the first time, an EV has been approved as a power plant for the German market. The monitoring and control of the loading and unloading processes are carried out for the EV to act as a regulatory reserve for the German electricity grid. Another project that was carried out through a partnership between Nissan, TenneT and The Mobility House used the EV *Nissan Leaf* as a way to store and save renewable energy in Germany (V2GHub, Access: 17 February, 2023).

The V2G control technology has yet to be regulated for real-world implementation and remains a new technology that requires many feasibility and impact studies (ABVE, Access: 12 December, 2022). In this way, the contribution of this article is the implementation of the V2G control in a real system through stimulation, which considers not only the medium voltage but also the low voltage. The simulation seeks to reproduce the user's consumption profile, stipulating an analysis of the results considering a significant insertion of EV in the system with medium and low voltage levels.

The paper is organized as follows: Section is divided into five parts: (i) Battery model, (ii) Converters model, (iii) System description, (iv) Electrical Vehicles Model (v) V2G Control technology. Section presents the simulation results. Finally, concluding remarks are presented in Section .

Theory and Method

Battery Model

The voltage of the Lithium Ion battery used in the EV is given by Equation 1(TREMBLAY, 2009).

$$V_{batt} = E_0 - K \frac{Q}{(Q - i_t)} i_t - Ri + A \exp(-Bi_t) - K \frac{Q}{(Q - i_t)} i_t(i^*)$$

(1)

Where,

- V_{batt} = Battery voltage (V);
- E_0 = battery constant voltage (V);
- K = Bias constant (V/Ah) or bias resistance (ohms);
- Q = battery capacity (Ah);
- i_t = idt integral = actual battery charge (Ah);
- A = Amplitude of the exponential zone (V);
- B = Inverse time constant of the exponential zone (Ah-1);
- R = Internal resistance (ohms);
- i = Battery current (A);
- i^* = Filtered current (A);

In the proposed battery model (TREMBLAY, 2009), the polarization resistance is represented by Equation 2, which represents the voltage characteristic that tends to increase rapidly when the battery reaches full charge. Thus, the resistance starts to increase abruptly from full load.

$$R_{Polarizac\tilde{a}o} = K \frac{Q}{i_t - 0.1 - Q}$$

(2)

The Lithium Ion battery discharge is given by Equation 3.

$$(3) \quad AExp(-Bi_t)$$

Briefly, the Equations that represent the behavior of the Lithium Ion battery for charging and discharging can be seen in Equations 4 and 5, respectively.

$$(4) \quad V_{batt} = E_0 - Ri - k \frac{Q}{i_t - 0.1Q} i^* - k \frac{Q}{Q - i_t} i_t + AExp(-Bi_t)$$

$$(5) \quad V_{batt} = E_0 - Ri - k \frac{Q}{Q - i_t} (i_t + i^*) + AExp(-Bi_t)$$

The definition of i^* is defined by the low frequency current, thus using a low pass filter. The definition of i_t is done by integrating the battery current that corresponds to the capacity drawn from the battery.

The SOC of the battery is defined through the Equation 6 (Porciuncula, 2012).

$$(6) \quad SOC = 100(1 - \frac{1}{Q} \int_0^t i(t) dt)$$

Converters Model

The battery is connected to the system through a two-stage converter, the first being a bidirectional current DC-DC converter (allowing bidirectional power flow) connected to a DC-AC inverter. Since the battery is in DC current and the system in AC current, the converter in this configuration acts as a grid support feature. In this way, it becomes possible to provide ancillary services through the control readings.

The definition of variable average value is given by Equation 7. The converter dynamics is described as a function of signal modulation. Differently from the Switched Model, the Average Model focuses on the dynamics of the average values of the variables, instead of the dynamics of the instantaneous values.

$$\bar{x}(t) = \frac{1}{T_s} \int_{t-T_s}^t x(\tau) d\tau \quad (7)$$

Equation 7 is applied in the Switched Model equations (Yazdani & Irvani, 2010). The result is Equations 8 and 9.

$$\bar{s}_1(t) = d \quad (8)$$

$$\bar{s}_2(t) = 1 - d \quad (9)$$

Furthermore, Equations 8 and 9 are replaced in the system of Equations that represent the Switched Model, so it is possible to obtain the Average Model as a function of the cyclical ratio. The AC voltage equation synthesized in the converter can be seen in 10. The Power Equations can be seen in 11, 12 and 13.

$$\bar{V}_t(t) = \frac{V_{DC}}{2} \cdot (2d - 1) \quad (10)$$

$$\bar{P}_{CC}(t) = \frac{V_{DC}}{2} \cdot (2d - 1) \cdot \bar{i}(t) \quad (11)$$

$$\bar{P}_t(t) = \frac{V_{DC}}{2} \cdot (2d - 1) \cdot \bar{i}(t) \quad (12)$$

$$\bar{P}_s(t) = V_s \cdot \bar{i}(t) \quad (13)$$

It is possible to determine a relationship between the cycle ratio of modulating signal magnitude "m" through the strategy used by the PWM, generating Equation 14.

$$d = \frac{m + 1}{2} \quad (14)$$

The set of Equations 15, 16, 17 and 18 represent the Average Model based on the magnitude of the modulating signal, which will be the main control variable (Yazdani & Irvani, 2010).

$$\bar{V}_t(t) = m \cdot \frac{V_{DC}}{2} \quad (15)$$

$$\bar{P}_{DC}(t) = m \cdot \frac{V_{DC}}{2} \cdot \bar{i}(t) \quad (16)$$

$$\bar{P}_t(t) = m \cdot \frac{V_{DC}}{2} \cdot \bar{i}(t) \quad (17)$$

$$\bar{P}_s(t) = V_s \cdot \bar{i}(t) \quad (18)$$

Based on Equations 15, 16, 17 and 18, the equivalent system is given in Figures 1 and 2.

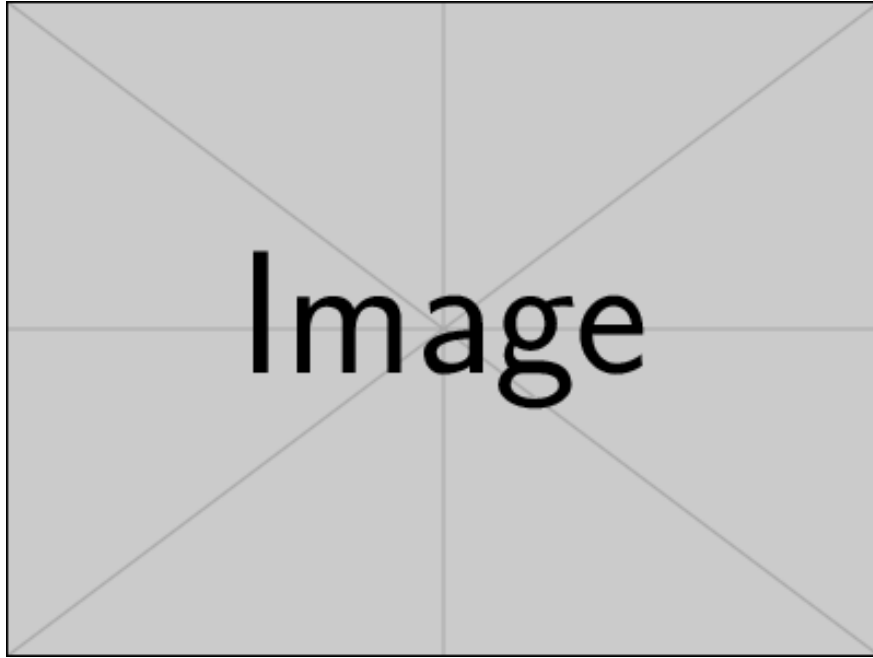


Figure 1: Simplified Power Circuit of the DC/AC half-bridge converter.

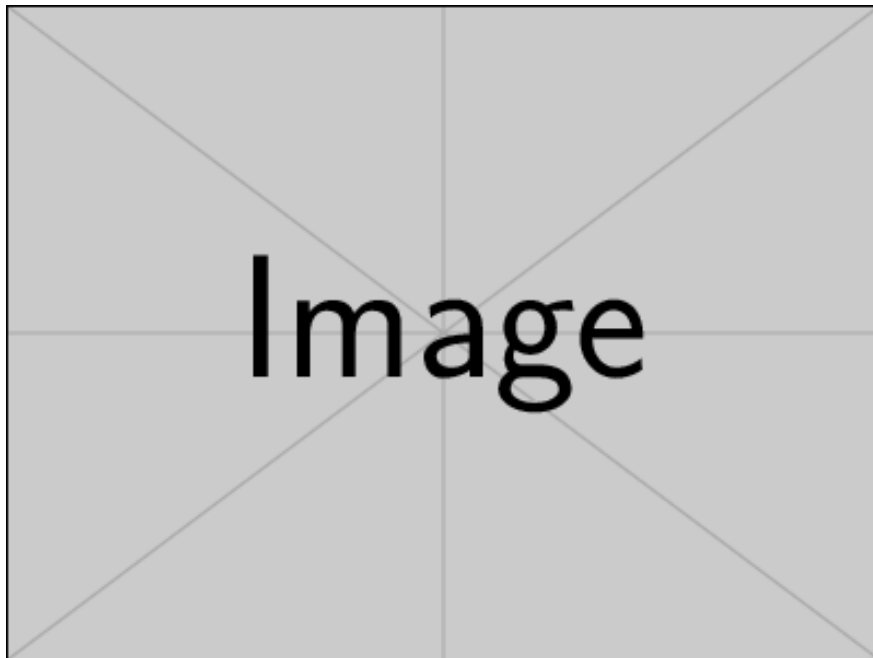


Figure 2: Average equivalent circuit of the half-bridge converter.

System Description

The distribution network studied comprises one region of the city of San José, the capital of Costa Rica. The modeled network can be seen in Figure 3 and the technical data specification can be seen in Table 1. The substation, low and medium voltage lines and distribution transformers are modeled based on a database provided by the local energy utility in Costa Rica. The data were made available through OpenDSS software, so the complete modeling of the network was started, performing the same in PSCAD software. The introduction of variant loads in the system was carried out with the aid of code developed in MATLAB software.

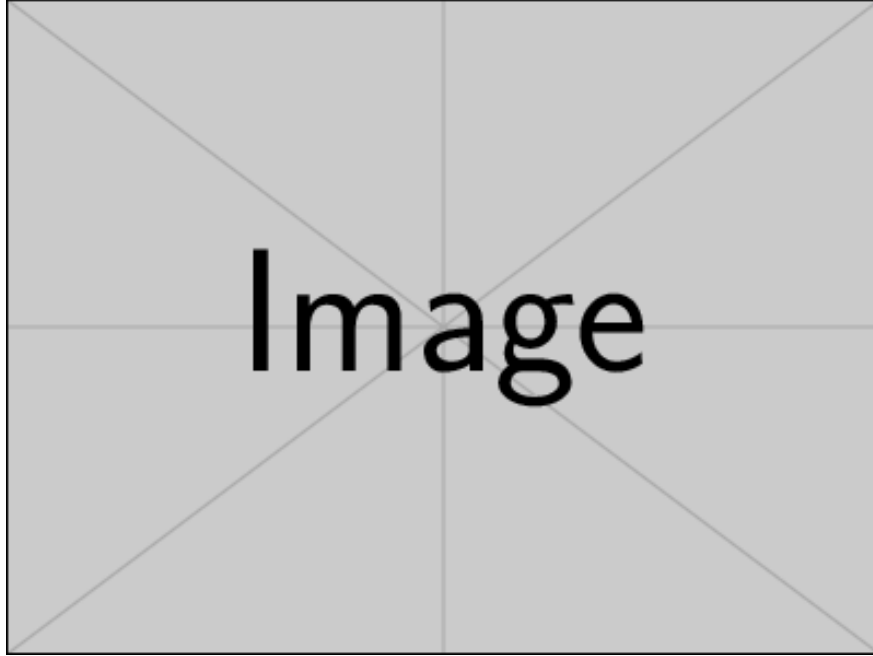


Figure 3: Case study topology of medium and low voltage distribution network.

Table 1: Technical data of the Distribution Network.
Costa Rica Distribution Network

Medium Voltage Line Level (kV)	34,5
Low Voltage Line Level (kV)	0,208
Number of Medium Voltage Lines	123
Number of Low Voltage Lines	1368
Number of Medium Voltage Buses	125
Number of Low Voltage Buses	1400
Number of Loads	654
Feeder Active Power (MW)	0,6299
Feeder Reactive Power (MVA _r)	0,0996
Substation Line Voltage Level (kV)	138/34,5
Rated apparent power (MVA)	0,6377
System extension (m)	17.554,60

The chosen network serves a total of 654 residential, commercial and industrial loads in Costa Rica. One example of load profile considered in this study is depicted in Figure 4.

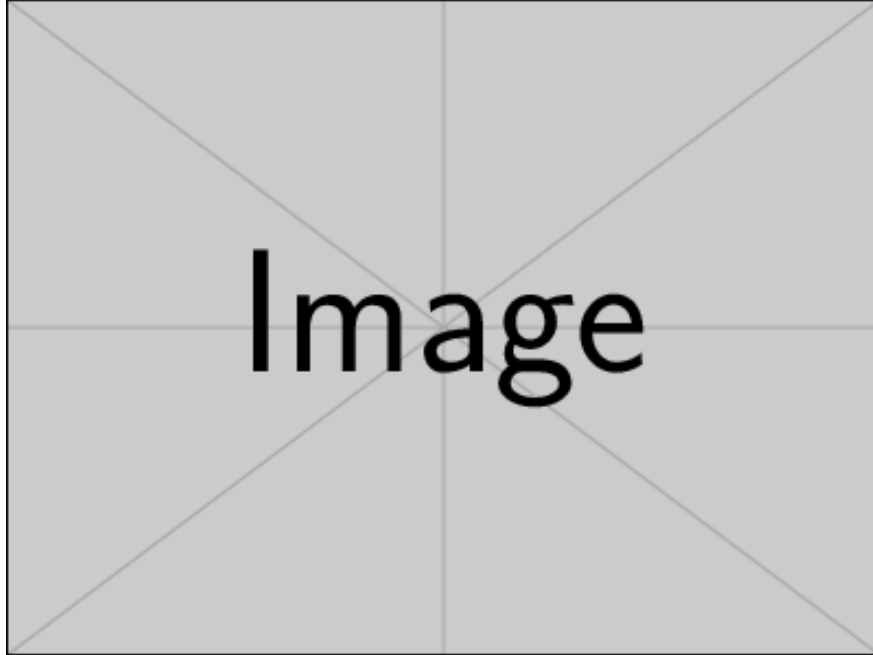


Figure 4: Real Load Curve.

Electric Vehicle Model

The Nissan Leaf model was chosen due to its wide use in the literature, as previously mentioned (Hayes & Davis, 2014) (Chukwu & Mahajan, 2013). Each Nissan Leaf has 40 kW of active power and a battery capacity of 115,942 A.h. The EVs were modeled to be connected to the low voltage of the three-phase system. The EV model was carried out aiming to be realistic, considering the load profiles and the social user's behavior that directly impact their connection/disconnection to the network.

In Figures 5 and 6, the modeling of the Lithium Ion battery from the Nissan Leaf model and the converters and the RL filter assembled in software PSCAD can be seen. Simulation parameters can be seen in Table 2. It is important to emphasize that the parameter values were obtained through projects focused on the development and construction of electric vehicles (Yazdani & Iravani, 2010) (*Contribuições ao estudo de conexão de sistemas fotovoltaicos a rede elétrica sem o uso de filtros passivos: projeto de controladores digitais para redução do conteúdo harmônico.*, 2013).

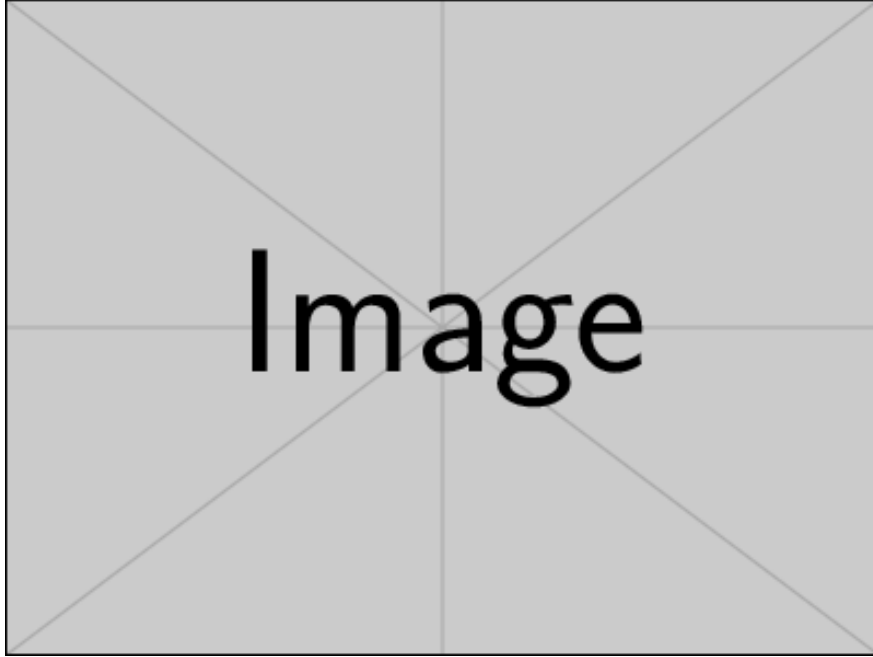


Figure 5: Battery model connected to a three-phase inverter in medium model.

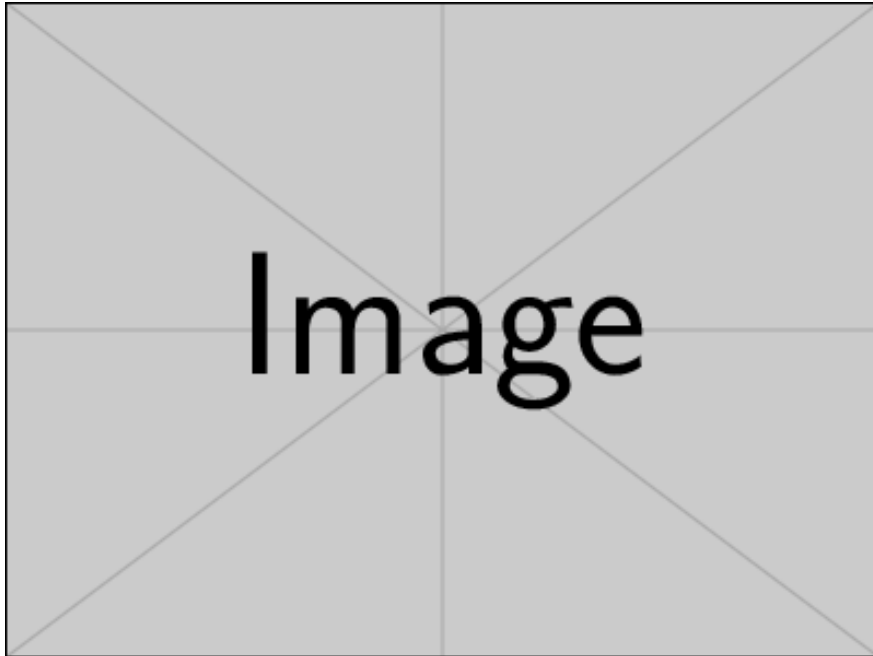


Figure 6: RL filter (internal to the inverter) at the point of common coupling implemented in PSCAD/EMTDC.

Table 2: Simulation parameters: Electric vehicles.

Circuit Elements	Description	Values
Controllers	DC Voltage Proportional Gain ($K_{Pv,bat}$)	0,5 $\frac{radF}{Vs}$
	DC Voltage Integral Gain ($K_{Iv,bat}$)	10 $\frac{radF^2}{Vs^2}$
	Proportional Current Gain ($K_{Pi,bat}$)	2 H/s
	Integral Current Gain ($K_{Ii,bat}$)	1 Ω/s
	Current controller time constant (τ)	0,5 ms
	Bidirectional Current Proportional Gain ($K_{Pi,bi}$)	3,3 H/s
	Integral Bidirectional Current Gain ($K_{Ii,bi}$)	33 Ω/s
	Current controller time constant Bi (τ)	1 ms
	Damping Factor (ξ)	0,7
	Cut Frequency (ω_n)	377 rad/s
	PLL current time constant (τ_{PLL})	4,5 ms
	PLL Cutoff Frequency ($\omega_{n,PLL}$)	628,3 rad/s
	PLL Proportional Gain ($K_{P,PLL}$)	3,7 rad/Vs
	Full PLL Gain ($K_{I,PLL}$)	685,39 rad/Vs^2
System Model	Voltage at the CCP (V_d)	120 V
	Frequency (f_s)	60 Hz
Bidirectional Converter	Input Filter Capacitor (C_{bat})	100 μF
	Input Filter Inductor (L_{bat})	3,3 mH
	Input Filter Resistance (R_{bat})	10 $m\Omega$
DC-AC Converter	DC bus capacitor (C_f)	1000 μF
	Output Filter Inductor (L_f)	1 mH
	Output Filter Resistance (R_{eq})	1 $m\Omega$
Time-Step	Power System ($Large - dt$)	100 μs

The type of charging chosen for the battery is semi-fast charging (AC Chargers Level 2) (de Arruda Bitencourt, 2022). The characteristics of the Nissan Leaf level 2 plug can be seen in Table 3, taking approximately 2 hours and 24 minutes to charge the EV battery, the SOC from 10% to 100%. Thus, the active power of the outlet of each EV is equal to 16,8 kW. In this way, the EV requests this maximum power from the network acting as a load, and during the V2G operation, each EV can supply the network with this maximum power value.

Table 3: Semi-rapid charging point characteristics of the *Nissan Leaf* model.

Type	SOC	Time	Electric Charging Point
Semi-fast charge	0% - 100%	~ 3 hours	240 V, 70 A

Four important topics were implemented to build the realistic EV model in the 24-hour simulations in PSCAD, as seen in the , , and .

Vehicles Average Load Curve

The EVs average load curve shown in Figure 7 was built in software MATLAB and implemented in PSCAD. The curve allows to understand the behavior of EVs users, informing the demand throughout the day, being built based on the literature review (Quirós-Tortós et al., 2018).

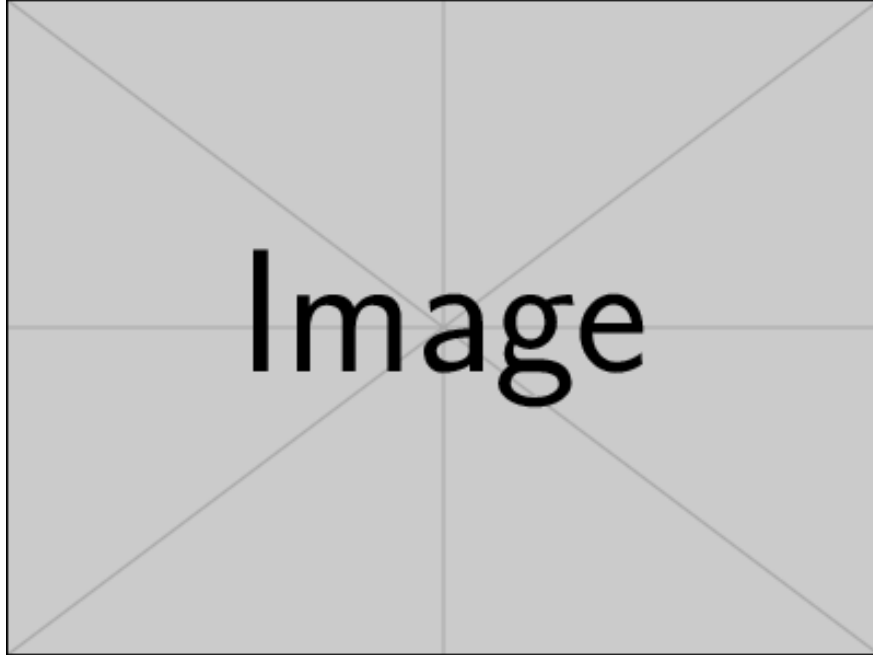


Figure 7: Electric Vehicles Load Curve.

The average curve is the result of extensive behavior research created through the MEA project (Quirós-Tortós et al., 2018). A characteristic behavior can be observed, since the load peak is at the end of the day, when the vast majority of users get home from work and charge their EVs. Also, during business hours, some users charge EVs while carrying out their work duties.

Connection and Disconnection Curves

To understand the behavior of the different user profiles, curves are needed to show when the battery will be connected/disconnected from the network, influenced by their daily lives. An ant colony algorithm, an optimization method, was developed in MATLAB to choose the best curves that represent the EVs connection and disconnection according to the users' characteristics to represent the average demand curve.

Basically, with the 1440 measurements (Quirós-Tortós et al., 2018) data on a weekday, containing the EVs connection and disconnection, the aim was to find 35 curves that combined are the best approximation of the average EVs curve for each minute. In this way, each solution was composed of 35 random curves. By calculating the error, the algorithm identifies the solutions that are most likely to represent the average curve based on the pheromone matrix. Though, the values tend to converge to a specific region of the problem. After a predefined number of iterations, 100 in the present study, the result represents the best solution found by the method (Dorigo et al., 2006) (Dorigo & Stützle, 2019).

An example is depicted in Figure 8. When the curve is zero, the vehicle is not connected to the network. On the other hand, the point where the curve is one represents that EV is connected to the network. It is worth noting that there is a tendency to increase the load towards the end of the day, with each color representing a user profile and their daily routine.

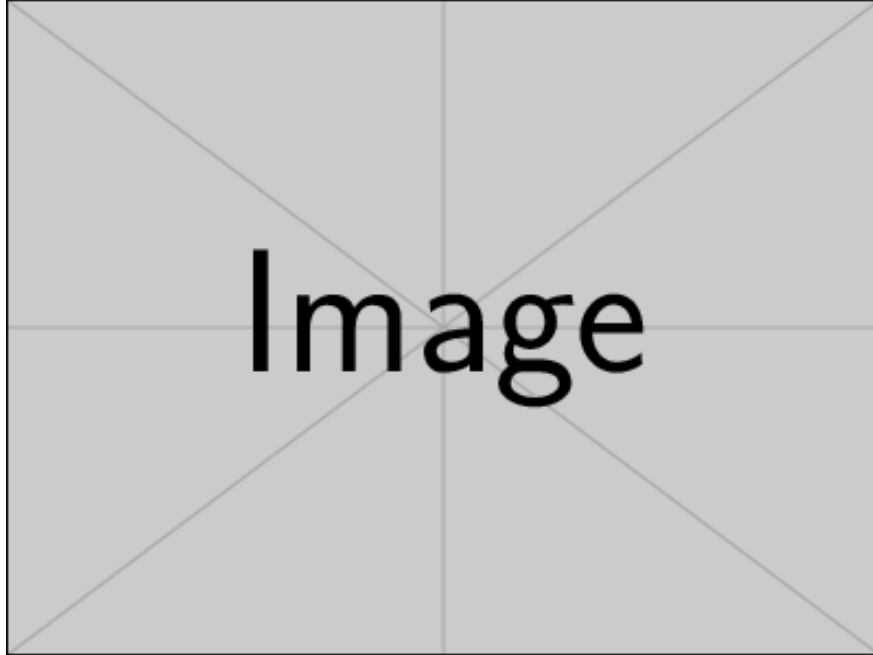


Figure 8: Connection/disconnection curve for different user profiles of the Nissan Leaf model.

Electric Vehicles and the grid power requirement

An important characteristic in the EV modeling is that the vehicles stop requesting power from the network when the vehicles are charged. Also, it must be considered that users charge their vehicle batteries at random SOC percentages throughout the day. To include this behavior into the simulations, a random number between 20% to 80% was randomly generated to represent the initial SOC of the EV connected to the network. This represents the routine of EV users. Figures 9 and 10 show the behavior of the SOC battery for the same users on two different days of the week.

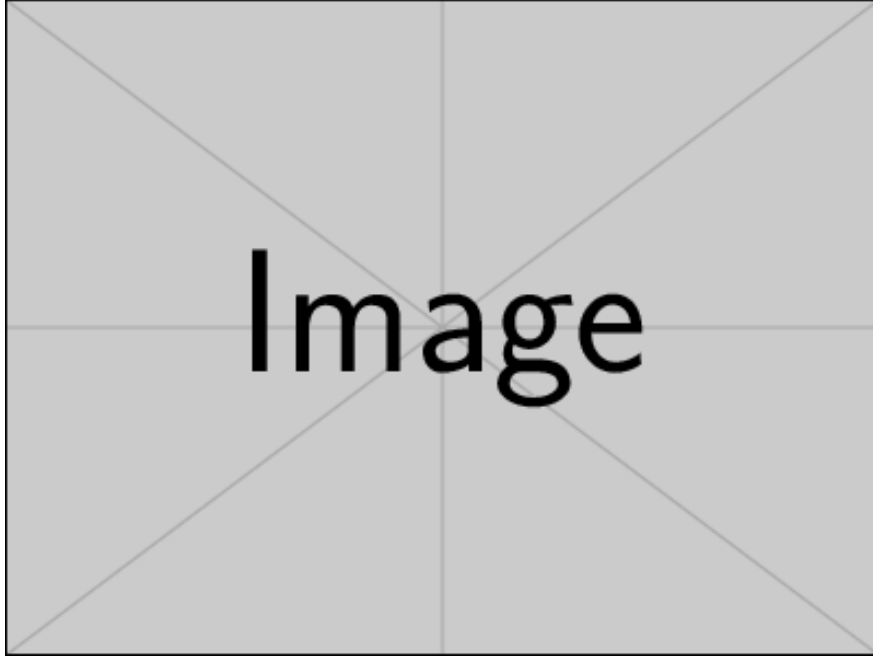


Figure 9: Five EVs battery SOC for different user profiles Nissan Leaf model – Day 1 of the week.

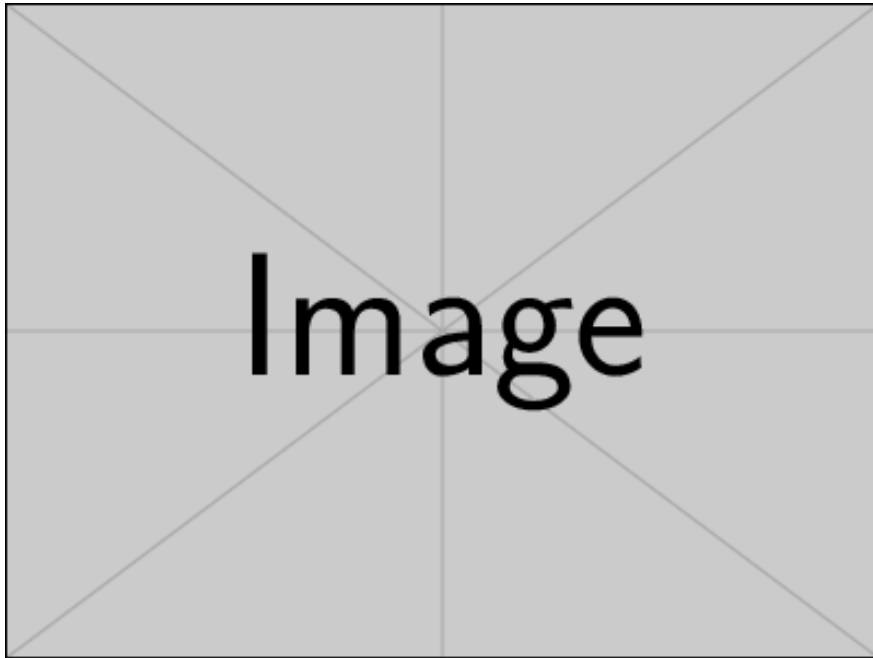


Figure 10: Five EVs battery SOC for different user profiles Nissan Leaf model – Day 2 of the week.

Vehicle battery discharge

The battery discharge modeling during the use of the EV by the owner is represented, thus modeling a complete cycle composed of charging and discharging the battery simulating a real behavior of the SOC profile

(Deotti et al., 2020) (Prado et al., 2021). A random number between 20% and the maximum percentage of the battery is drawn when the batteries are disconnected, thus representing the state of charge that the battery will reach for the next charge. In this way, a more complete and faithful simulation of the user's probabilistic reality is built, representing the users profile. Figures 9 and 10 show this behavior.

V2G Control Technology

The integration of the V2G technology in a smart grid requires a bidirectional power flow controller as a decision-making mechanism (an inverter was used to allow the bidirectional flow) to the EV performance as a mitigating element or as a system load. The EVs ability to act as a mitigating element depends entirely on the state of the renewable and non-renewable energy generating units and the SOC of each EV, in other words, the technical characteristics of the network and the vehicle. Furthermore, the user's decision-making is crucial, being dependent on the purpose of using the EV, so the user may or may not allow the V2G control to work. In general there are conditions that must be met, if and only if these conditions are true, the EV can act using the V2G technology. Among these simulation constraints, the following can be mentioned:

- **Connection to the charging point:** The first condition is the EV be connected to the charging point while the V2G control is operating, this is given by the curves for different user profiles of the Nissan Leaf model, exemplified in Figure 8.
- **User authorization :** To implement this condition a binary number was randomly drawn in order to have 80% chance that the user would allow V2G to act (when the binary drawn is number one) and 20% chance of the user would not allow the V2G operation (when the binary drawn is number zero). These percentages were chosen to increase the chances of observing the performance of V2G in the results.
- **Vehicle SOC :** If the state of charge of the vehicle's battery is below a defined percentage of SOC the control V2G will not act. This condition is important to ensure battery life, reliability and user safety. The percentage chosen is 30%. It is worth mentioning that if, during V2G operation, SOC reaches a value of 30%, it will oscillate between loading and unloading the vehicle.
- **Voltage Control :** The V2G will only work at times of peak load (high demand). A comparison of different voltage readings is performed in order to evaluate the results. The reading will be carried out at the PCC and on the secondary of the three-phase medium voltage to low voltage transformer, to which the EVs connection bus is downstream.

Each simulation run approximately 7 hours in Core i7 7th Generation computer, Inspiron 14 P74G DELL. The V2G input data are the time, reading point voltage and outlet power reference, while the V2G output data are the V2G actuation decision: power reference output and the status, as can be seen in Figure 11.

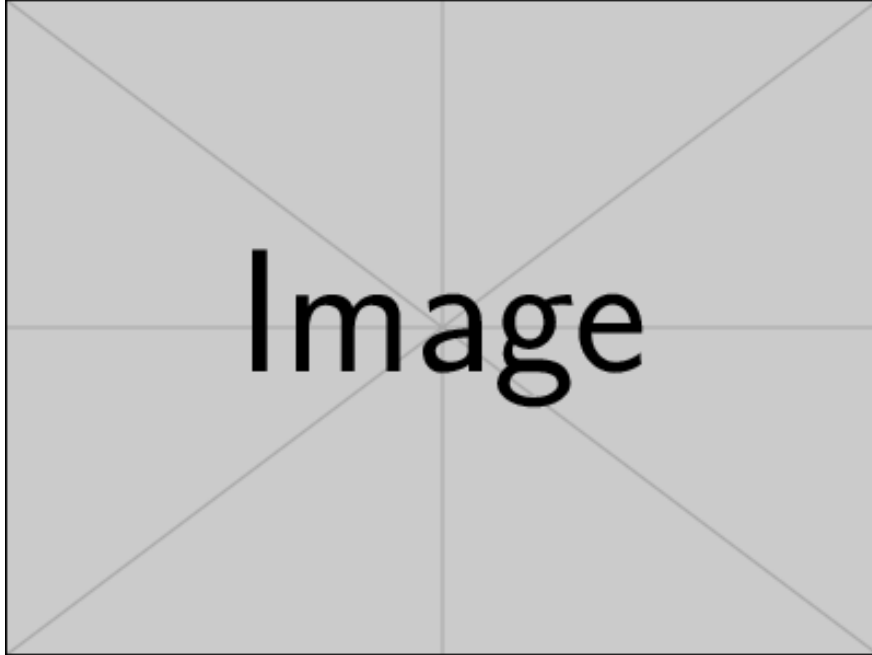


Figure 11: The V2G input and output.

The Droop curve that can be seen in Figure 12 is used to define how much power the EV will make available to the network according to the value of the network voltage reading. The delivered power is the required power, and the value is limited by the maximum power of the plug to which the EV is connected.

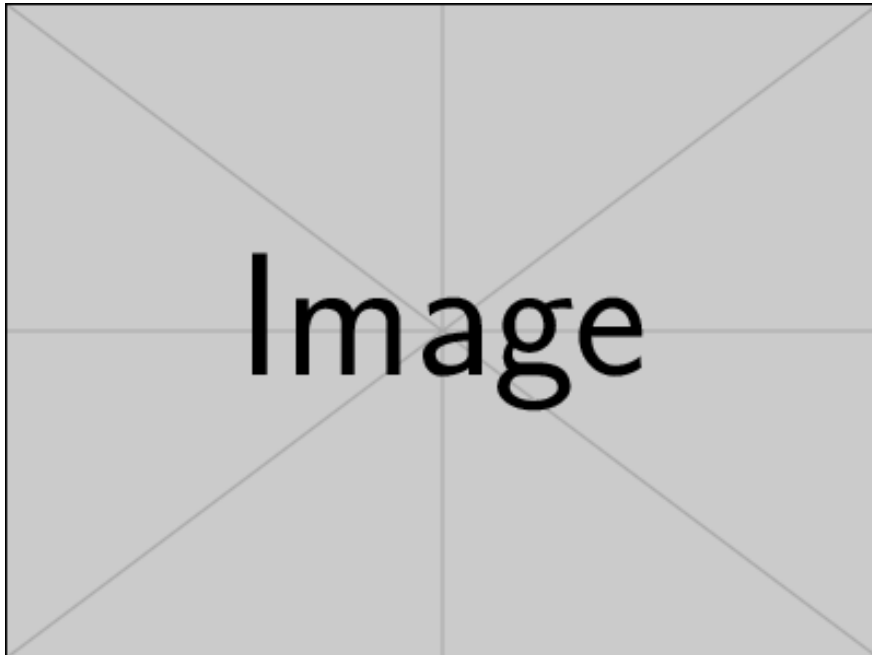


Figure 12: Droop Curve.

It can be seen that the maximum power from the plug will be delivered to the grid when the voltage values are between 0,87 pu and 0,92 pu. For values greater than 0,92 pu and less than 0,97 pu, the power value delivered through V2G will be proportional to the voltage reading. If the voltage is greater than 0,97 pu, even if the user allows the use of V2G and all the previously mentioned conditions are met, EV will charge normally, acting as a load.

Results and Discussion

The focus of this study is to evaluate the performance of the V2G technology in different EVs allocation scenarios, aiming at understanding the behavior of the system with the insertion of this technology. The voltage readings performed by the V2G control will be tested for the PCC of the EV plug and at the secondary of the medium to low voltage transformers adjacent to the connection buses of the EV plug. In order to facilitate understanding, Figure 13 didactically shows the difference between the two V2G control reading points in a simplified system. The simulations are run in PSCAD over 24 dynamic hours, with a simulation step of 100 μ s.

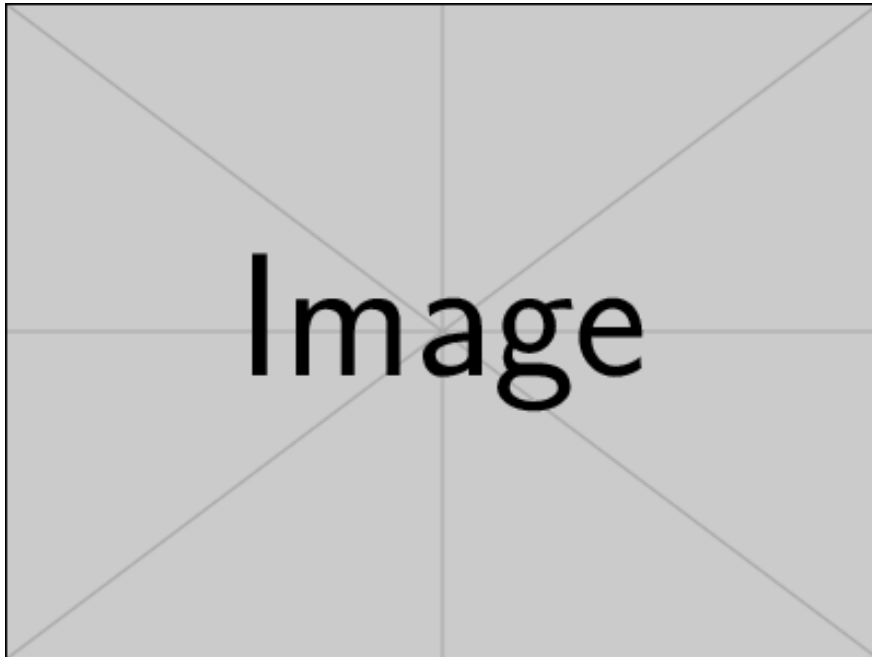


Figure 13: The difference between the two V2G control reading points.

It is known that, in general, the location of the charging points is carried out in places where there are users, so the EVs allocation has an unpredictability and randomness characteristic. The EVs allocation is determined by heuristic, but with a strategic thought out in order to connect the EVs in sensitive and non-sensitive buses.

In this work, sensitive buses are defined as the buses that are more likely to have undervoltage, since they are located further downstream in the system, away from medium to low voltage transformers. Non-sensitive buses are defined as those closest to the transformers, therefore, buses that are less likely to have undervoltage issues. It is worth mentioning that the EV modeling was carried out for the three-phase low voltage part of the Costa Rica system.

Therefore, predicting the allocation of EVs is not straightforward, and understanding the network topology becomes crucial to differentiate between sensitive and non-sensitive buses. The results of the chosen study cases aim to contemplate this characteristic to show the behavior of the network in face of a considerable insertion of EVs. Three cases will be analyzed:

- **First Case:** Is the base case, the system simulation without EVs;
- **Second Case:** Simulation of the system with 30 vehicles implemented in non-sensitive buses. Subsequently, insertion of the V2G control with two different voltage readings;
- **Third Case:** Simulation of the system with 30 vehicles implemented in sensitive and non-sensitive buses. Subsequently, insertion of the V2G control with two different voltage readings;

It is important to emphasize that for the same routine of a EV user there are different network power demands when considering different days of the week. The generated undervoltage will depend on the SOC percentage of the vehicle battery, so it is important to consider different SOC percentages to understand the level of technical problems that a real network can have when we add the EV as a load. The EV users can start the day with high or low SOC percentages, this randomness is included in the results for a better understanding of network behavior.

First Case

First, the Base Case is simulated. The analysis is important to understand the behavior of the system before and after EVs inserting, understanding the load characteristics. Figure 14 shows the system demand curve, being measured on the secondary side of the substation. The average voltage in the secondary of the substation can be seen in Figure 15.

The bus voltages of the system can be seen in Figure 16, the maximum and minimum voltage limits are given by Table 4 (Medium Voltage) and by the Table 5 (Low Voltage). There is no extrapolation of voltage levels regarding overvoltage or undervoltage, according to the regulations of the module 8 of the PRODIST (ANEEL, Access: 24 December, 2022). The red lines in Figure 16 highlight these limits visually. It is worth mentioning that there was no voltage extrapolation in the medium voltage buses in any case.

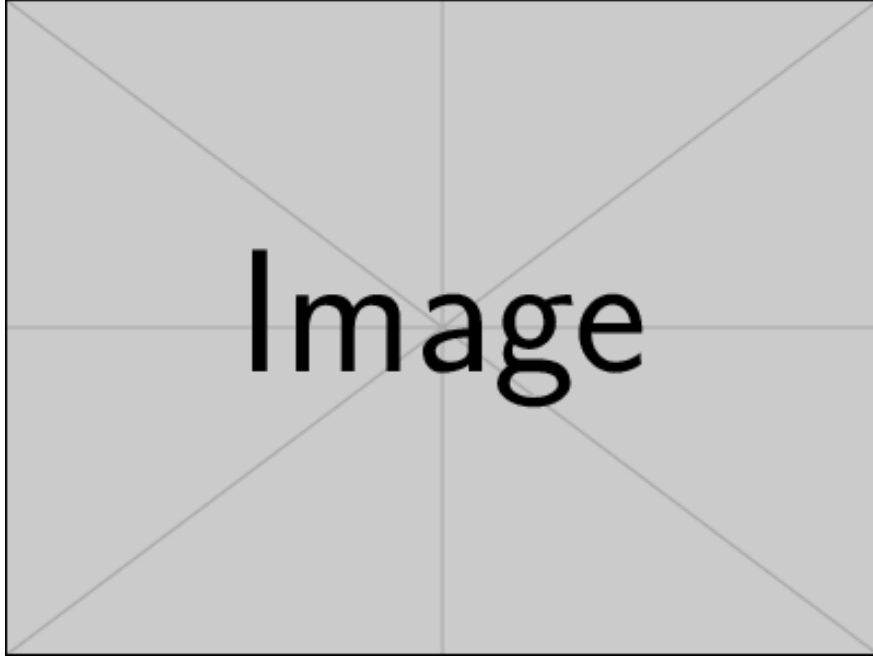


Figure 14: Costa Rica system demand.

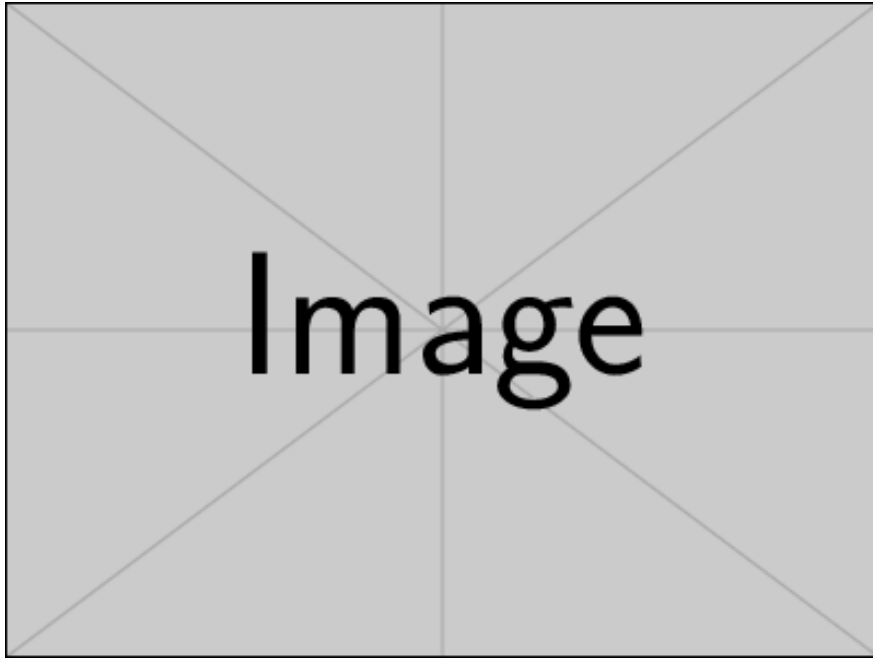


Figure 15: Voltage in the secondary of the Costa Rica system substation - Medium Voltage.

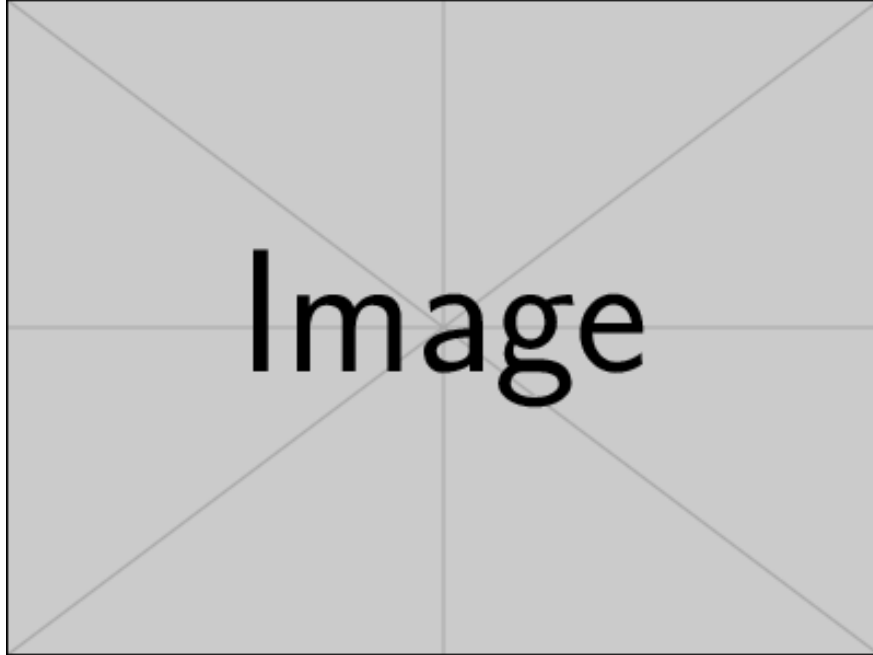


Figure 16: Costa Rica System voltage profile implemented in PSCAD/EMTDC (each color represents a system bus).

Table 4: Service Voltage Classification for 1KV_iV_i69KV. (ANEEL, Access: 24 December, 2022) Reading Voltage (TL) and Reference Voltage (TR).

Service Voltage (TA)	TL Variation Range in relation to TR
Proper	0,93 TR ≤ TL ≤ 1,05 TR
Precarious	0,90 TR ≤ TL ≤ 0,93 TR
Critic	TL < 0,90 TR or TL > 1,05 TR

Table 5: Service Voltage Classification for V_i1kV. (ANEEL, Access: 24 December, 2022) Reading Voltage (TL) and Nominal Voltage (TN).

Service Voltage (TA)	TL Variation Range in relation to TN
Proper	0,92 TN ≤ TL ≤ 1,05 TN
Precarious	0,87 TN ≤ TL < 0,92 TN or 1,05 TN < TL ≤ 1,06 TN
Critic	TL < 0,87 TN or TL > 1,06 TN

Second Case

It is interesting to understand the behavior of the system when the EV are connected in non-sensitive buses of the system, that is, the buses that are closer to the medium voltage transformers for the low voltage. Such buses allow a greater number of EV connected to the network, consequently a greater number of users.

In this way, 10 blocks were implemented each containing 3 grouped EVs, totaling 30 Nissan Leafs, equivalent to 85,83% penetration in the system. The vehicle’s semi-fast plugs have 16.800 W, so each block when connected to the grid consumes 50.400 W. It is noteworthy that the installed load of the EV is 1,2 MW, as each Nissan Leaf is characterized by 40.000 W.

The buses that were connected to the blocks of EV can be seen in Table 6. The buses voltage is 120 V.

Table 6: Characteristics of EV allocation buses - Second Case.

System Buses	Distance from the nearest Transformer (m)
BUSLVFLX1107.1.2.3	54,3442
BUSLVFLX1219.1.2.3	45,6651
BUSLVFLX1203.1.2.3	49,1399
BUSLVFLX1143.1.2.3	46,7618
BUSLVFLX1135.1.2.3	31,1134
BUSLVFLX1275.1.2.3	9,4079
BUSLVFLX25.1.2.3	0,0000
BUSLVFLX1278.1.2.3	9,4068
BUSLVFLX1279.1.2.3	9,0931
BUSLVFLX1288.1.2.3	9,3735

The demand curve of the system for the Second Case can be seen in Figure 17, and the corresponding voltages of the low voltage buses can be seen in Figure 18.

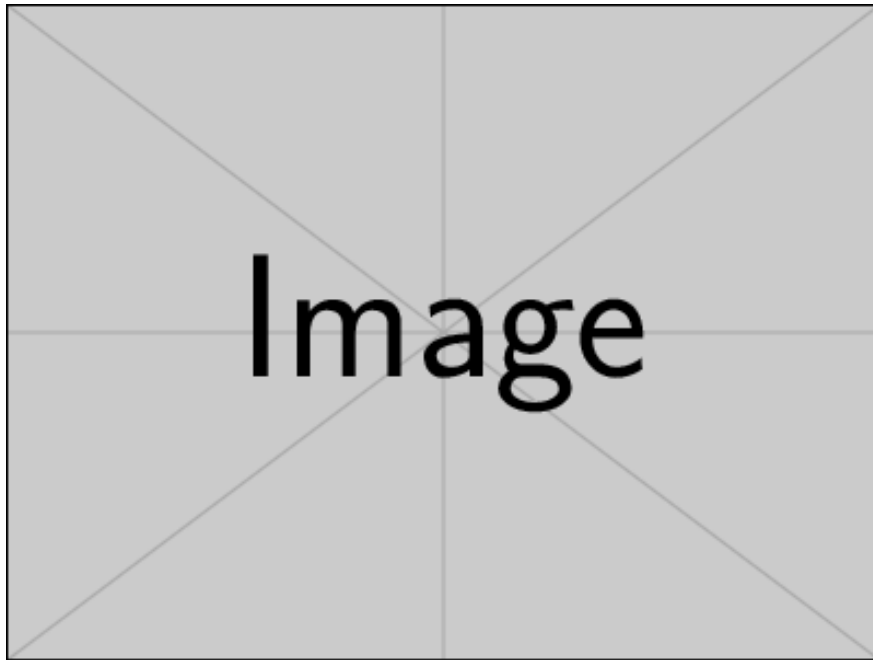


Figure 17: System demand with the insertion of EV - Second Case.

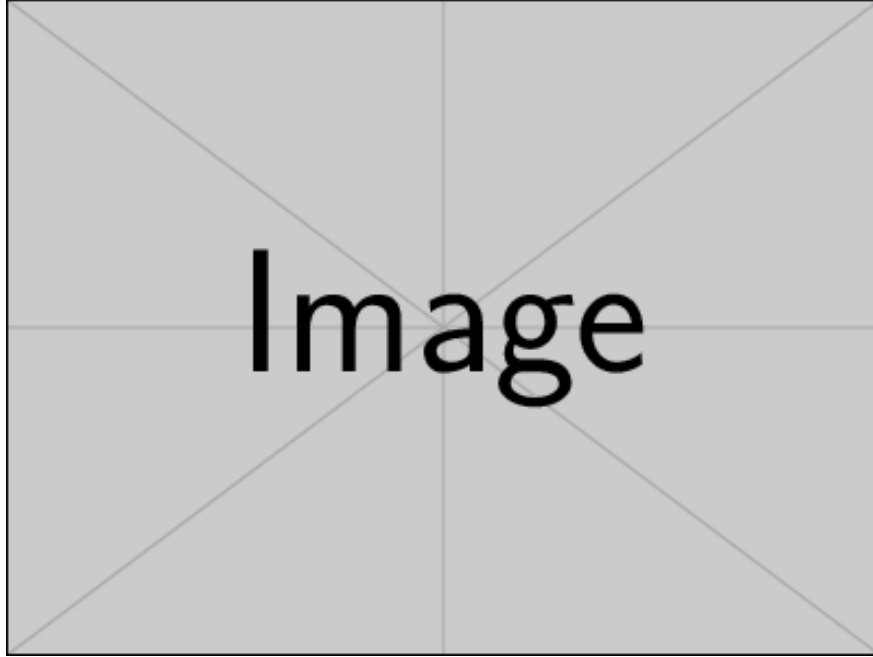


Figure 18: Low Voltage Profile of the Costa Rica System (each color represents a system bus) - Second Case.

As for the system's demand, there is an even more pronounced load peak from 6 PM to 8 PM after the insertion of 85,83% penetration of EV. The undervoltage is milder because it is close to 0,92 pu, occurring from 4:15 PM to 5:15 PM and approximately 7:40 PM. Despite the high penetration, during the rest of the day voltages behaved within the range considered adequate.

The Active Power demanded by the 10 blocks of 3 EV to the grid can be seen through Figure 19, added together they correspond to 504 kW of power connected to the grid. When the active power demanded by the vehicles requires active power, the EV are loaded, behaving like a load in the system. The SOC behavior of each block of EV on a typical weekday for different user profiles can be seen in Figure 20. It is observed that most users charge their vehicles later in the day, as expected and seen in the voltage and power profile.

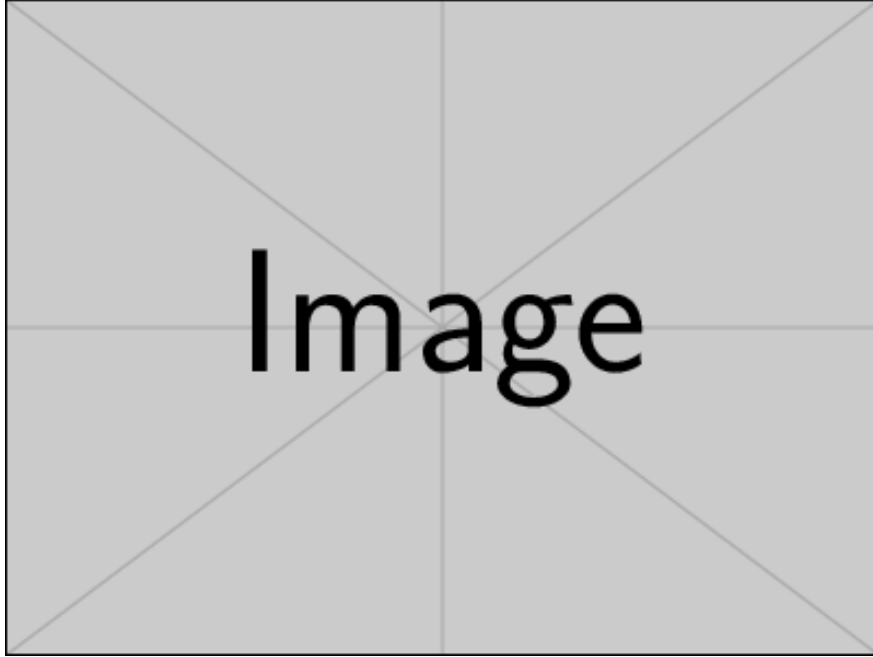


Figure 19: Three-phase active power demanded by each block of EV - Second Case.

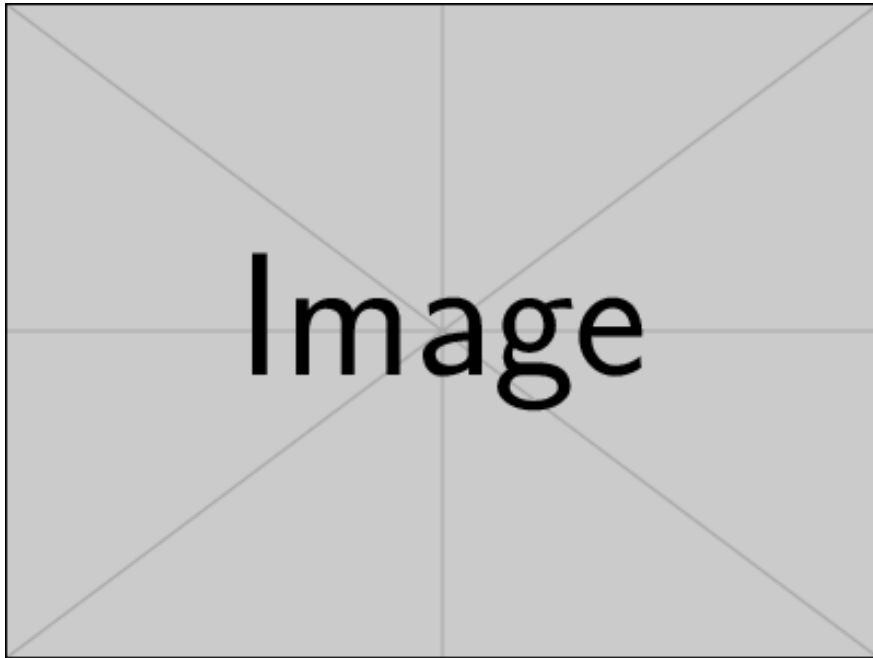


Figure 20: SOC of the battery of each block of EV - Second Case.

V2G control at the PCC - Second Case

The system's Active Power measured on the secondary side of the substation can be seen in Figure 21. It is observed that the V2G performance is clear in the shape of the curve, indicating in certain areas that

the control acted in such a way that EV supplied the network, no longer acting as a load, but rather as an ancillary service, injecting active power into the grid. The control acted in a way that the demand drastically reduced in the peak hour, from 6 PM to 8 PM.

In Figure 22, the Droop Curve chosen allows the V2G technology to act proportionally in voltages between 0,92 pu and 0,97 pu, and to act with maximum power in voltage values below 0,92 pu, for this reason, the low voltage buses have the voltage corrected to values within the observed spectrum. These values are between the red dotted curves, indicating that after V2G actuation with voltage reading at the PCC, no undervoltage is observed in the system.

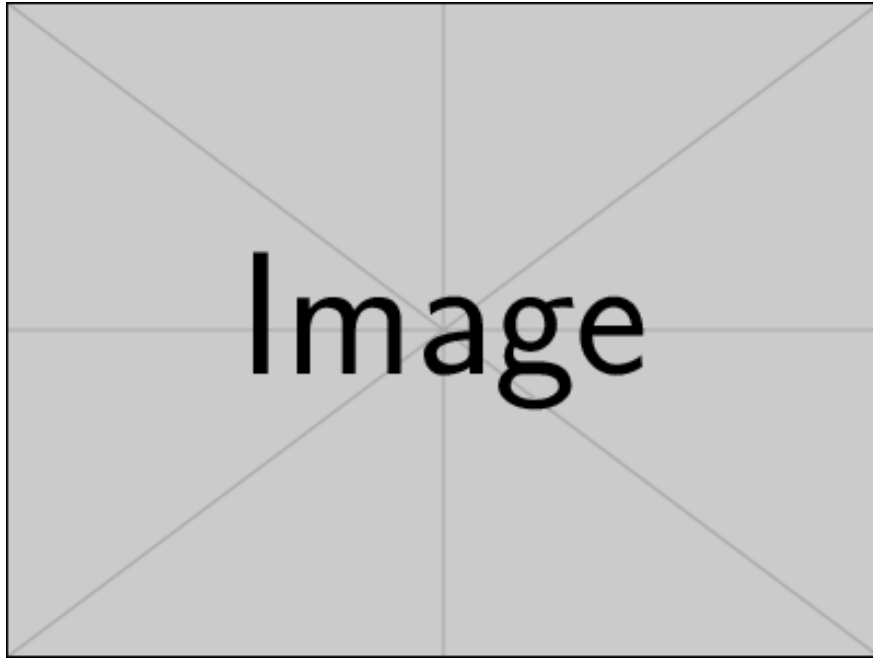


Figure 21: System demand with the insertion of EV after V2G control at the PCC - Second Case.

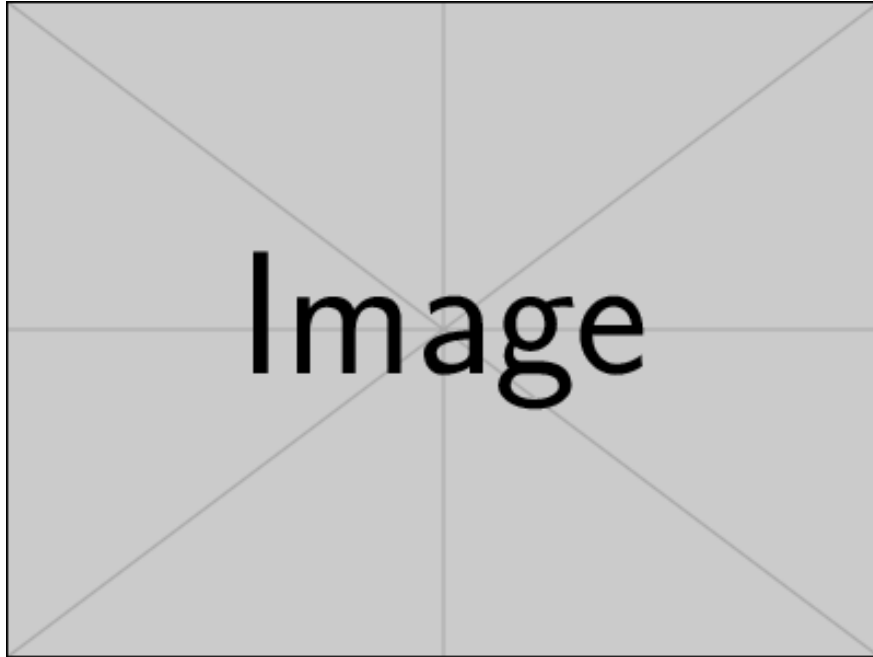


Figure 22: Low voltage profile of the Costa Rica System with V2G control at the PCC (each color represents a system bus) - Second Case.

The three-phase Active Power reading at the PCC of the EV sockets can be seen in Figure 23. It is noteworthy that the power curves with oscillatory characteristics are characterized by the ancillary service, in other words, the EV injecting power into the network. Figure 24 shows the SOC behavior, characterizing this oscillatory behavior to provide the necessary power to the network according to the undervoltage levels presented at certain times of the day.

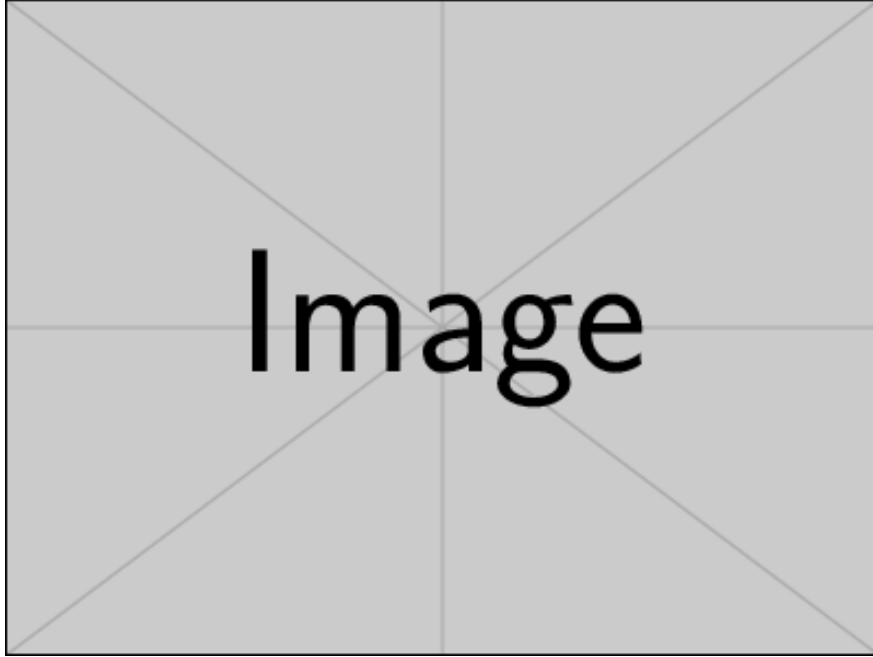


Figure 23: Reading of three-phase active power in the EV plugs after V2G control at the PCC - Second Case.

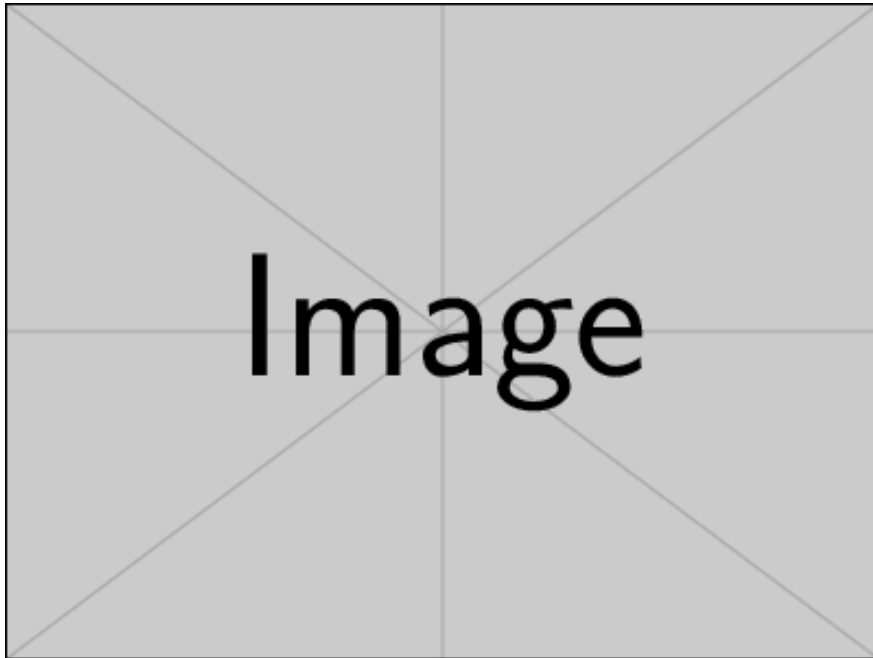


Figure 24: SOC from the battery of each block of EV after V2G control at the PCC - Second Case.

V2G control at the transformer - Second Case

The performance analysis of the V2G control with reading on the medium to low voltage transformer, closer to the buses that are connected to the EV outlet, was carried out to understand and compare the two different control readings.

The power demand of the system for this case can be seen in Figure 25. The required power of the system at peak hours is reduced, in addition to an oscillatory characteristic seen between 4 PM and 5 PM, which corresponds to the performance of the control during undervoltage hours.

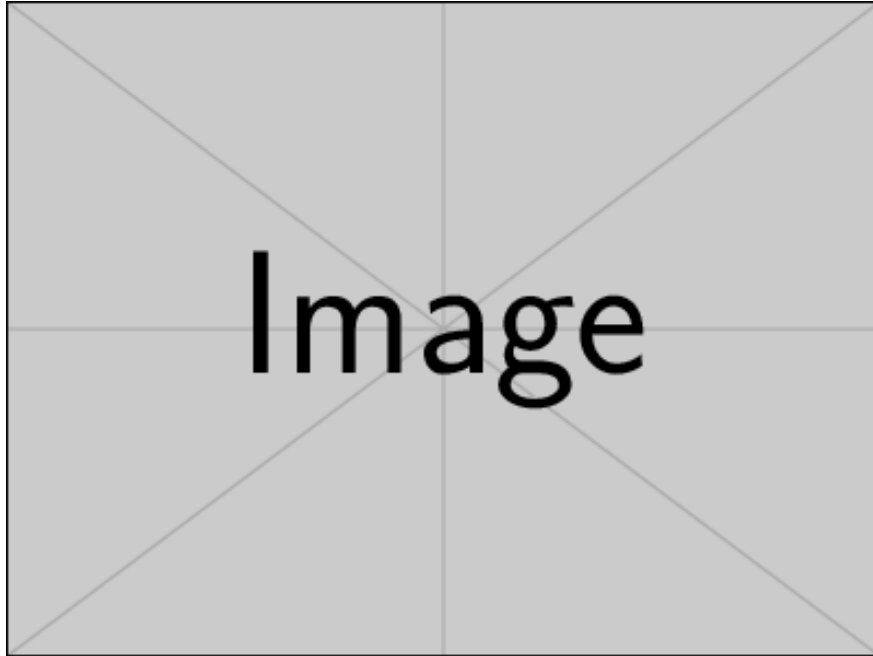


Figure 25: System demand with the insertion of EV after V2G control at the transformer - Second Case.

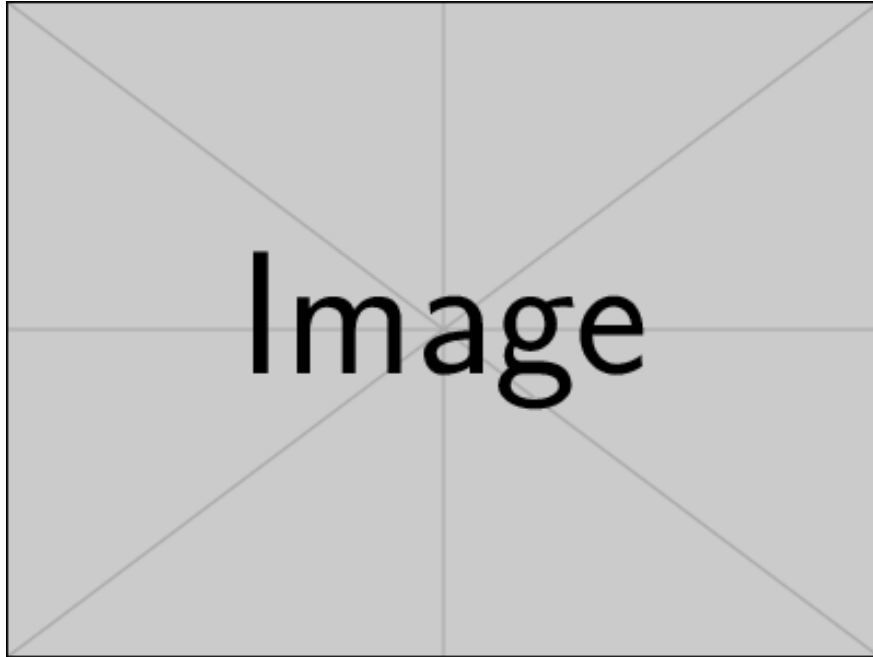


Figure 26: Low voltage profile of the Costa Rica System with V2G control at the transformer (each color represents a system bus) - Second Case.

Figure 26 shows the voltages of the low voltage buses. The V2G control reading for this case was successful, so the EV injected the power that the system needed. The conservative characteristics of the Droop curve contributed since the V2G control acts proportionally up to 0.97 pu. It was strategically thought out because Costa Rica's system proved to be a more sensitive system.

Figure 27 shows the active power reading of the EV outlets. Figure 28 shows the SOC of the vehicle batteries. The moments of power injection by the EV batteries, in other words, the actuation of the V2G control can be observed as small oscillations in the purple and red curves in the system, proving to be a case with a small level of undervoltage that requires little power for technical mitigation.

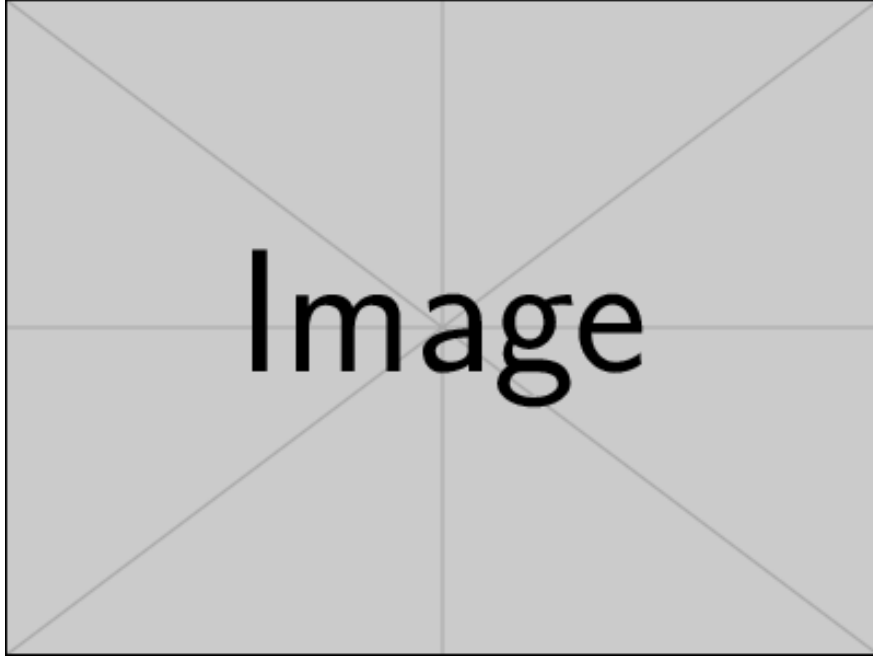


Figure 27: Reading of three-phase active power in the EV plugs after V2G control at the transformer - Second Case.

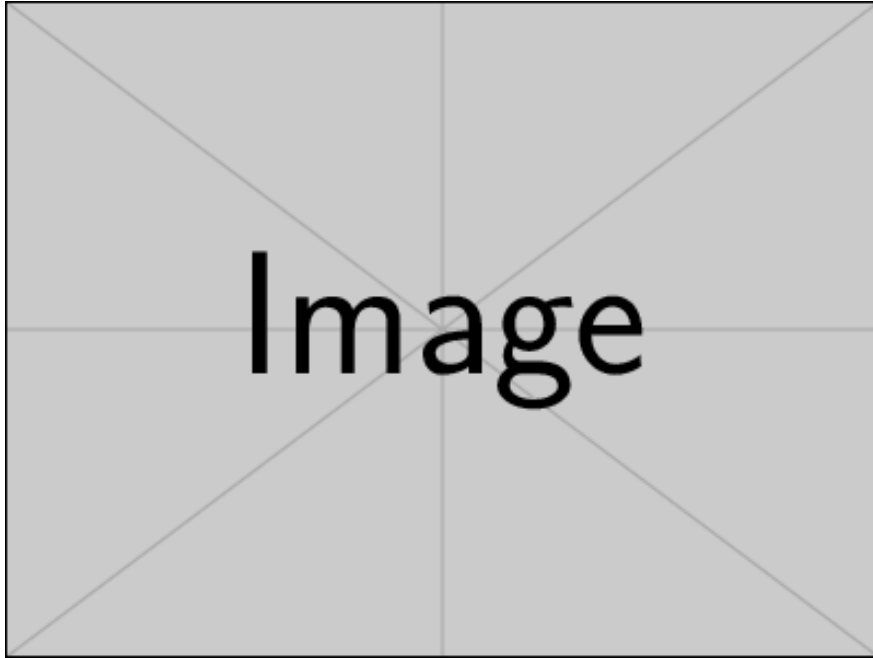


Figure 28: SOC from the battery of each block of EV after V2G control at the transformer - Second Case.

Third Case

It is known that in a real network the EV allocation is carried out in positions not expected by the distributor since the outlets are installed in places where there are users, so the allocation has this unpredictability characteristic. The Third Case aims to contemplate an allocation in sensitive and non-sensitive buses of the system in order to have the same percentage of power penetration as the Second Case. In this way, 10 blocks were implemented each containing 3 grouped EVs. The idea is to deal with a case with undervoltage in order to see the clear performance of the V2G technology in the substantial insertion of EV, in addition to demonstrating that the allocation buses have great importance in the response of the system.

The buses that were connected to the blocks of EV can be seen in Table 7. The buses voltage is 120 V.

Table 7: Characteristics of EV allocation buses - Third Case.

System Buses	Distance from the nearest Transformer (m)
BUSLVFLX1207.1.2.3	166,5435
BUSLVFLX1265.1.2.3	84,0045
BUSLVFLX1237.1.2.3	61,4560
BUSLVFLX1270.1.2.3	85,0832
BUSLVFLX1169.1.2.3	7,8662
BUSLVFLX1391.1.2.3	9,1493
BUSLVFLX1389.1.2.3	9,4893
BUSLVFLX1292.1.2.3	9,4118
BUSLVFLX1290.1.2.3	9,4167
BUSLVFLX1283.1.2.3	9,4134

In the low-voltage buses, which can be seen in Figure 30, a greater load is observed towards the end of the day, thus impacting the demand curve, seen in Figure 29, in those moments that are required from the large power network. The observed undervoltage levels are higher when compared to the Second Case, as it reaches 0,83 pu.

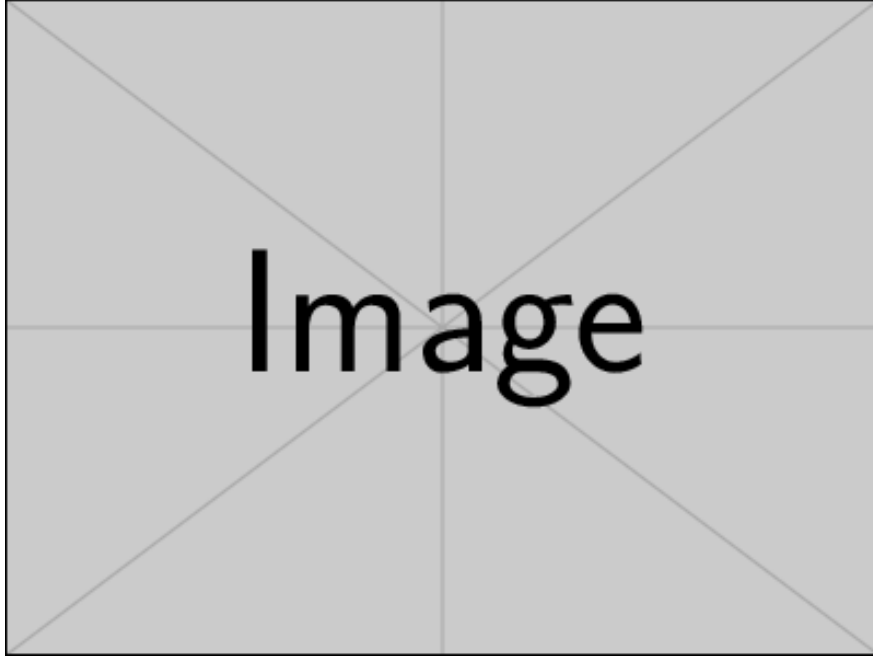


Figure 29: System demand with insertion of EV - Third Case.

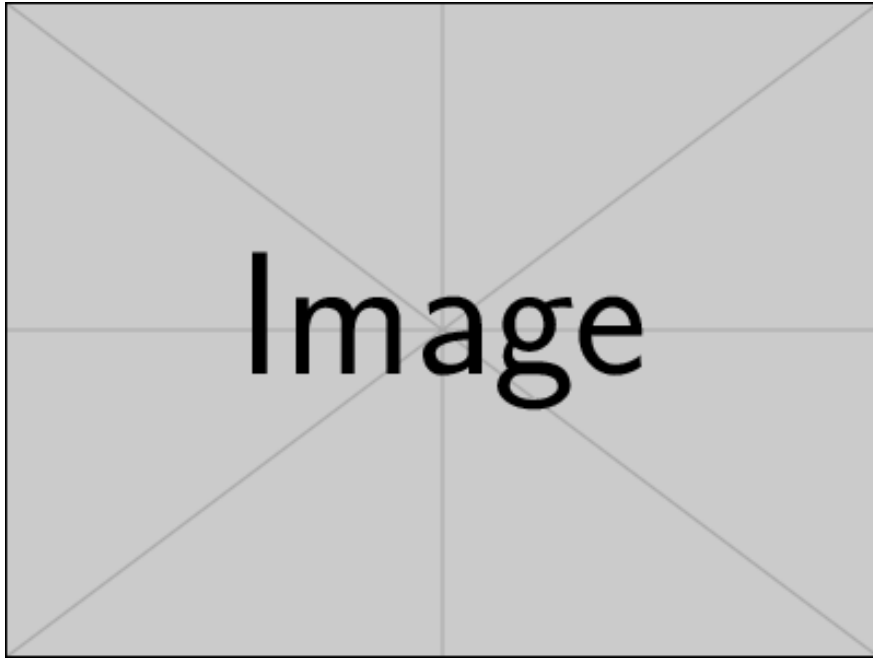


Figure 30: Low Voltage Profile of the Costa Rica System (each color represents a system bus) - Third Case.

The active power demanded by the 30 EVs to the network can be seen through Figure 31. The SOC behavior of each block of EV on a typical weekday for different user profiles can be seen in Figure 32.

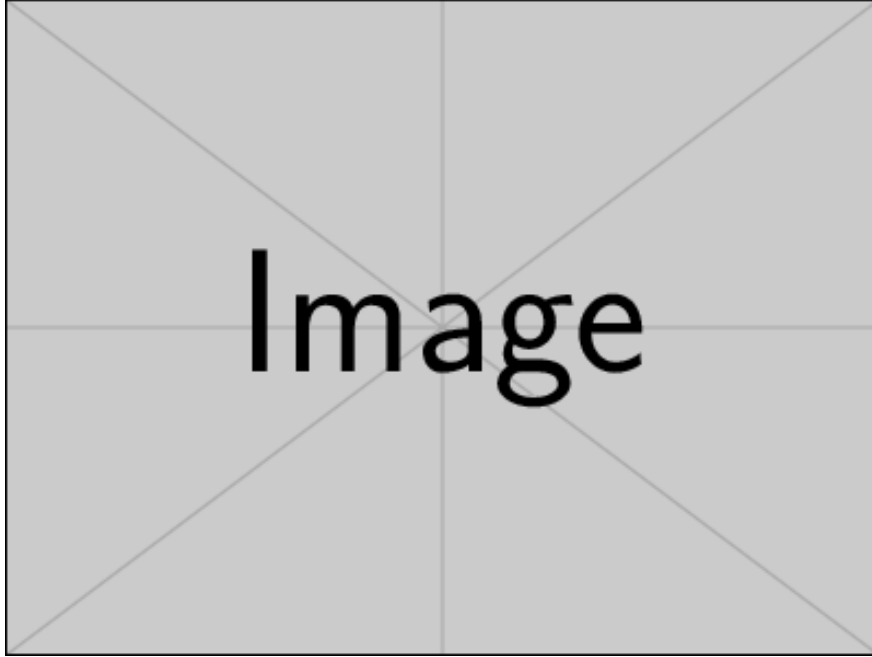


Figure 31: Three-phase active power demand for each block of EV - Third Case.

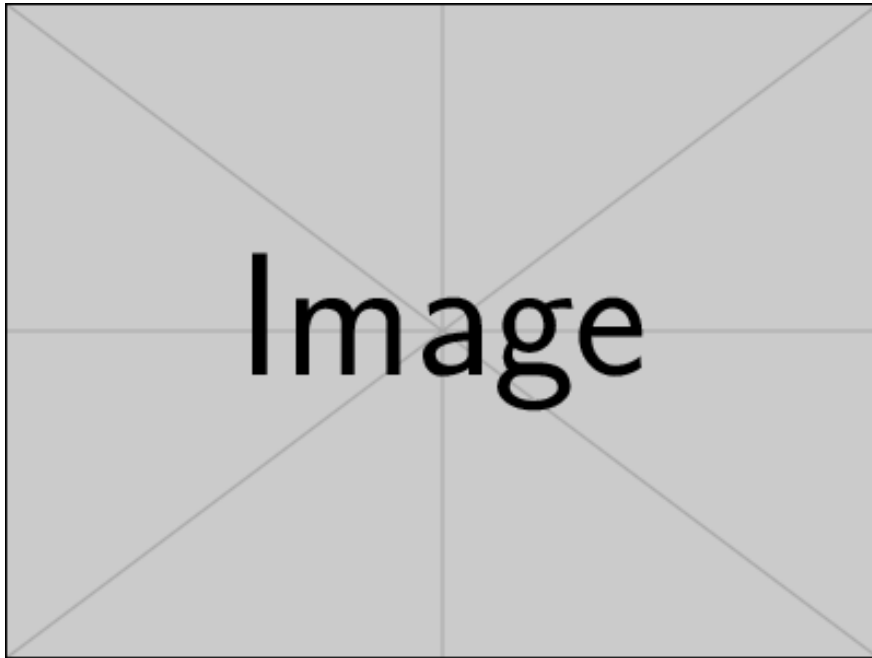


Figure 32: SOC of the battery of each block of EV - Third Case.

V2G control at the PCC - Third Case

Bearing in mind that the Third Case demands a lot of power from the system at peak hours, which are times that demand planning from the distributor to supply via generation even when there is no insertion of EV,

the V2G technology will be implemented in the system as a proposal to mitigate undervoltage.

The effect of the V2G control on the system's demand curve can be clearly seen in Figure 33. The oscillatory characteristic perceived at certain moments of the curve is due to the performance of the control, it is noticed that at these moments there is a decrease in demand. In Figure 34 can be seen that the undervoltage was successfully exhausted at several points, especially in the most critical case of undervoltage verified on the case before the control actuated, between 9 PM and 10 PM.

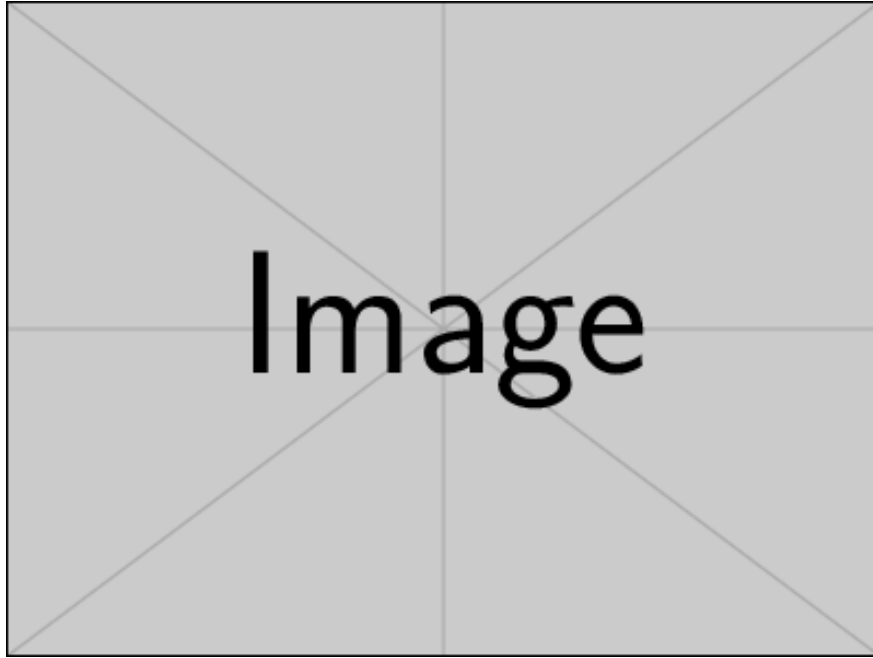


Figure 33: System demand with the insertion of EV after V2G control at the PCC - Third Case.

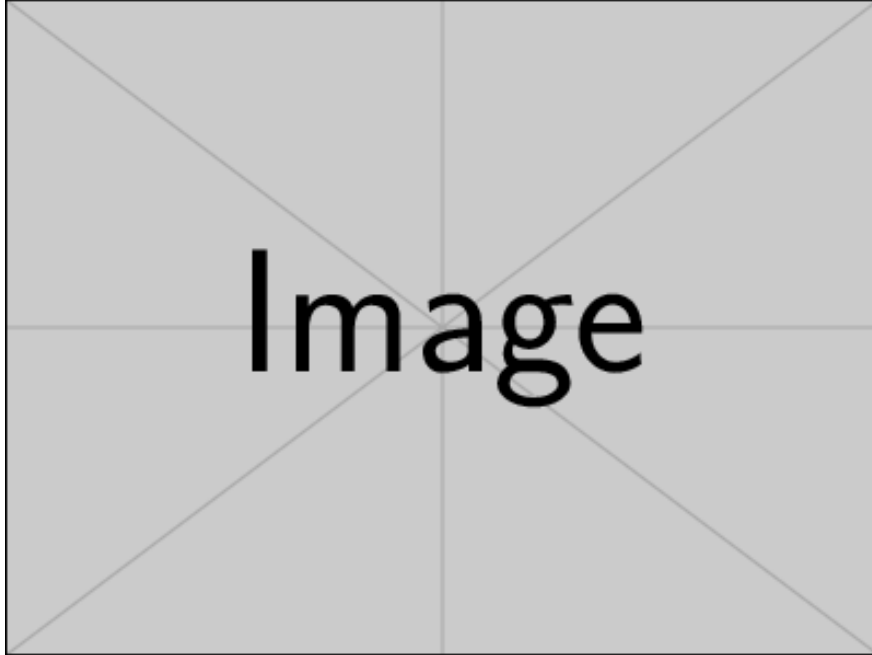


Figure 34: Low voltage profile of the Costa Rica System with V2G control at the PCC (each color represents a system bus) - Third Case.

In Figure 35 there is a tendency for the curves to move towards the positive power axis, after V2G actuation, but the same does not occur, as the loading characteristic is greater, because the power delivered is proportional to the voltage reading, oscillating between charging and discharging the battery as seen in Figure 36.

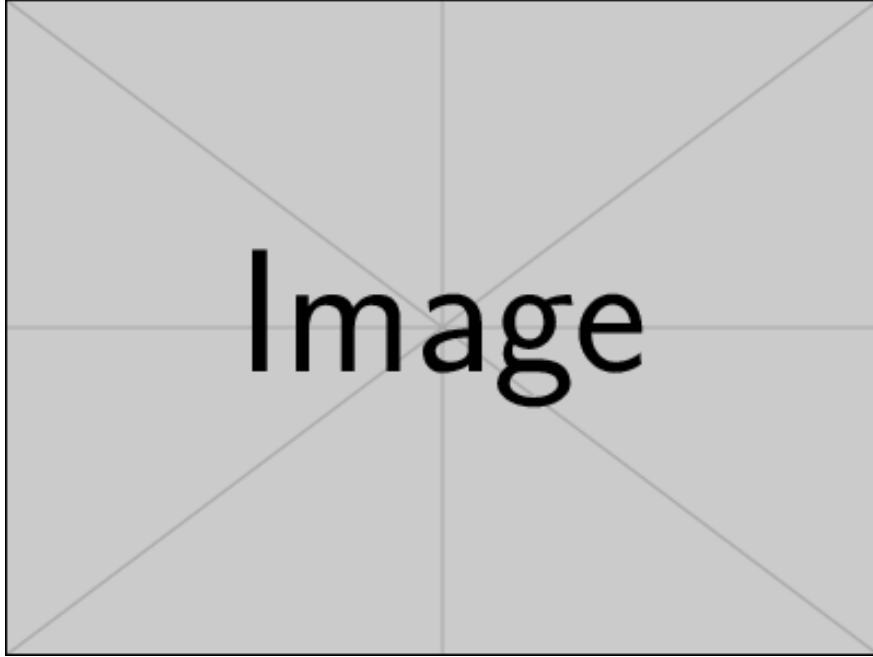


Figure 35: Reading of three-phase active power in the EV plugs after V2G control at the PCC - Third Case.

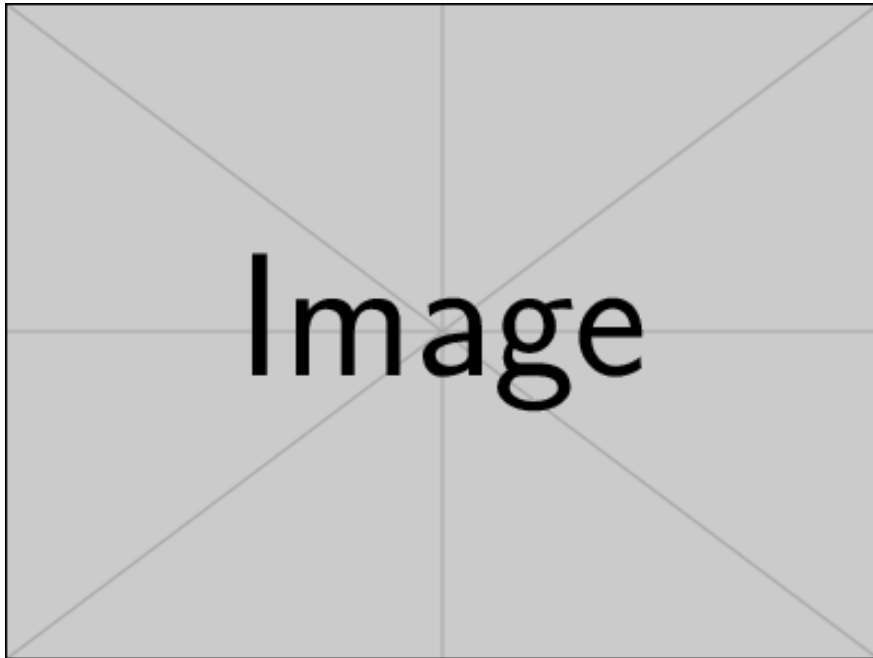


Figure 36: SOC from the battery of each block of EV after V2G control at the PCC - Third Case.

V2G control at the transformer - Third Case

The system demand after actuation of the V2G control with reading at the transformer can be seen in Figure 37. Note that just by modifying the voltage reading buses, the control acts in a completely different way from the previous case, instead of contributing by injecting power to reduce the demand, the demand intensifies in the peak hours from 6 PM to 8 PM. This can be explained by observing Figure 38, which presents the low voltage curves of the system for this control reading.

Furthermore, observing Figure 30 from 6 PM to 8 PM to compare with Figure 38, it can be seen that the undervoltage is more intensified in the latter. This is due to the initial conditions of the SOC that differ, for the case of EV acting as a load, during this period the battery's SOC initialized at a high percentage (the user used the vehicle little previously), thus providing a lower absorption of energy from the system, for a shorter time, causing a smaller undervoltage. In the case of V2G actuation with transformer readings, the battery's SOC for that period initialized lower (the user had used the vehicle a lot previously), demanding more power from the system, resulting in a dip of higher voltage.

In addition, the reading is carried out on the secondary of the transformers gives the chance that the control V2G will not act, since it does not see a large part of the system that is after the reading point, and they are exactly the buses farthest from the transformers, tend to be more sensitive and allow for greater undervoltage. So there may be worse cases beyond that point and they are not considered.

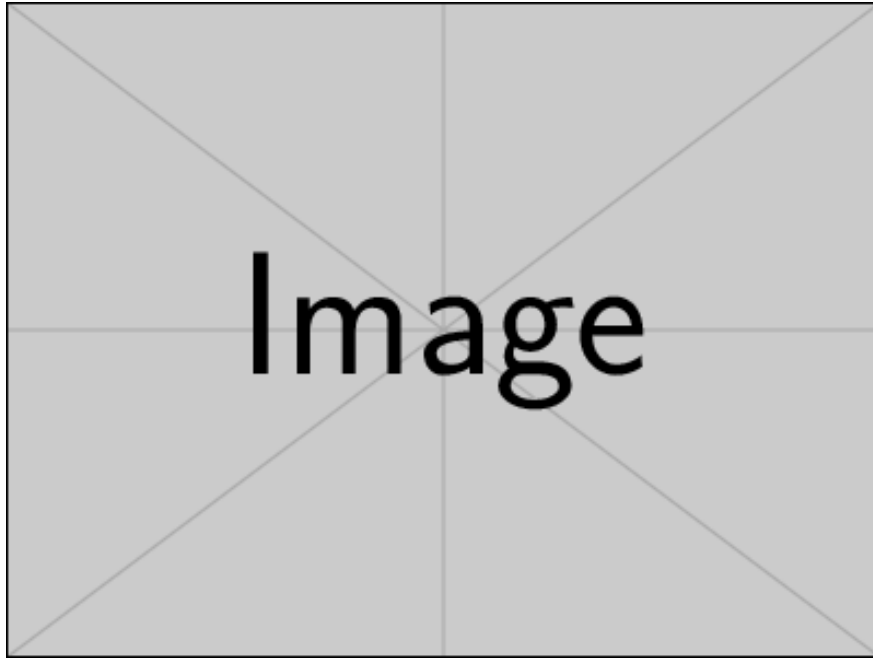


Figure 37: System demand with the insertion of EV after V2G control at transformer - Third Case.

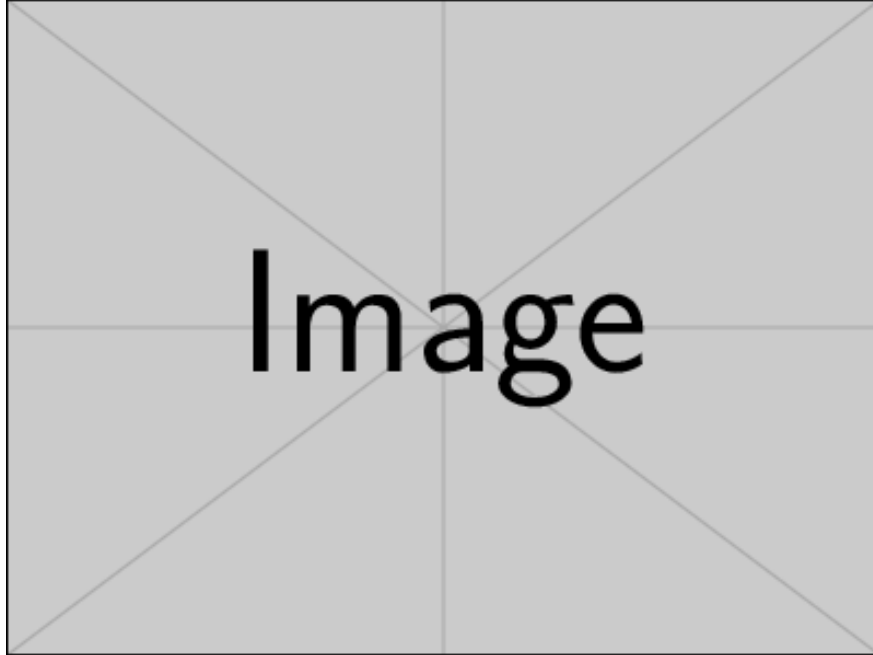


Figure 38: Low voltage profile of the Costa Rica System with V2G control at transformer (each color represents a system bus) - Third Case.

Observing the behavior of the low voltage buses in Figure 38, it can be concluded that the V2G reading on the medium to low voltage transformer did not act to exhaust or considerably reduce the undervoltage. The reading did not prove to be interesting as a way of acting as an ancillary service for the network. Figures 39 and 40 show V2G's attempt to mitigate the undervoltage in order to modify the active power curves seen by the EV outlet, and try to inject power, as seen in the SOC behavior, but the reading did not allow the control to act in the best way, according to the needs of the downstream transformer buses.

It is interesting to observe Figure 41 which shows the readings of the monitoring buses, which correspond to the secondary of the transformers. Clearly, no undervoltage is observed in Bus 25 and Bus 26 where the control performed the reading, proving what was explained in the previous paragraphs.

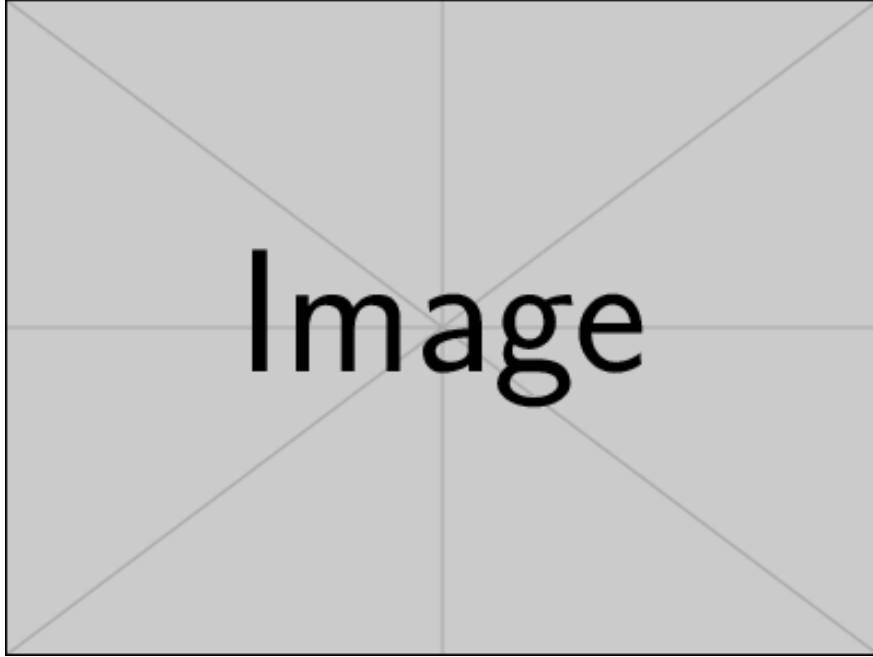


Figure 39: Reading of three-phase active power in the EV plugs after V2G control at the transformer - Third Case.

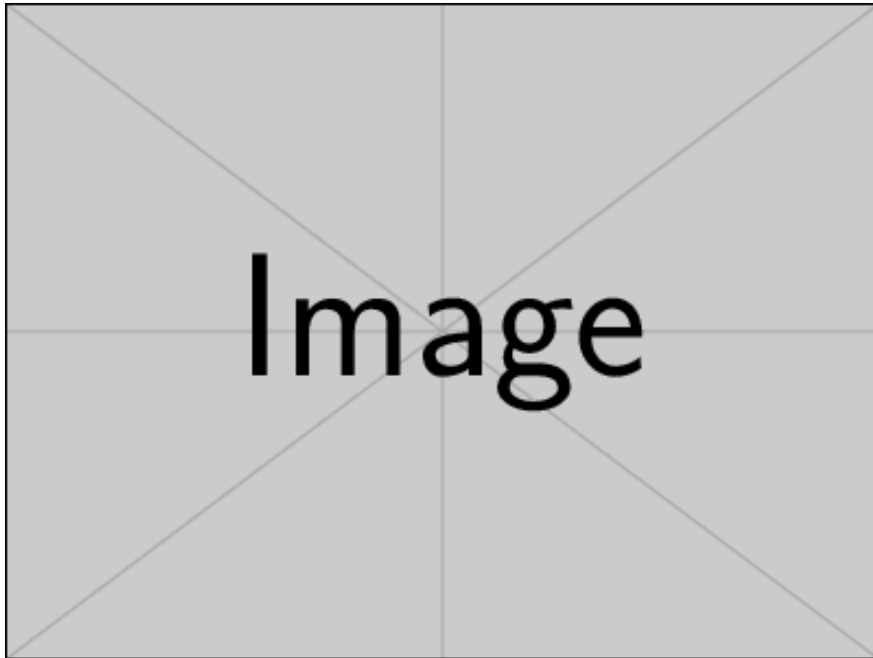


Figure 40: SOC from the battery of each block of EV after V2G control at the transformer - Third Case.

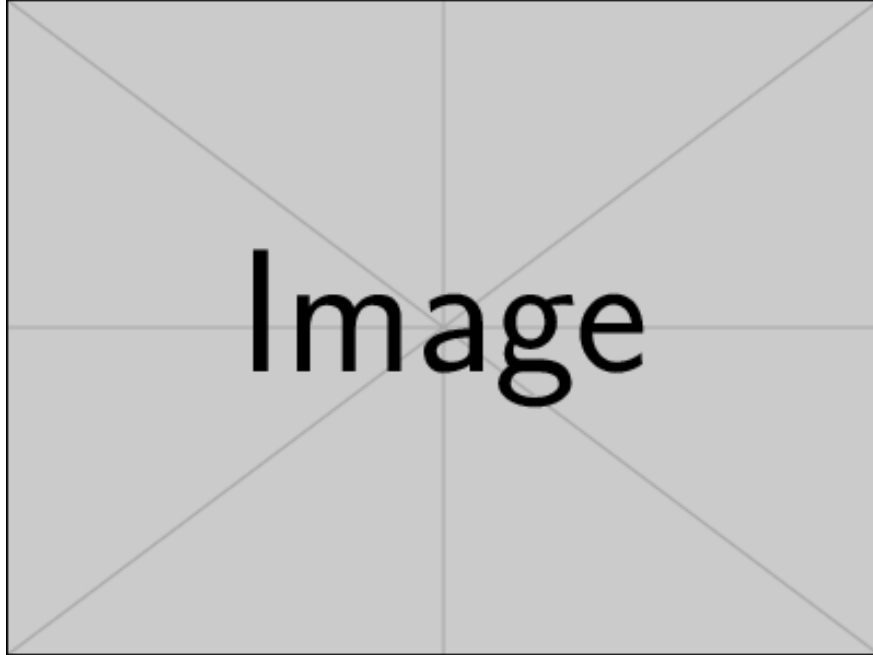


Figure 41: Buses voltage profile monitored in the V2G control of the Costa Rica System with V2G control at the transformer - Third Case.

Conclusion

This work focuses on the analysis of technical effects of EVs penetration in a real network. By understanding these effects, it is possible to propose mitigation procedures. This study evaluates the application of V2G control techniques, comparing the results for the voltage reading at the PCC and at the medium to low voltage transformers upstream of the EVs outlet buses.

The analysis makes use of an EVs average model, based on the Nissan Leaf model, considering real consumption profiles of users and dynamic load profiles. The objective is to validate and analyse the effects on the chosen network, which operates at 60 Hz, 34,5 kV (Medium Voltage) and 0,208 kV (Low Voltage). Simulations are performed in PSCAD with hourly resolutions and the results are presented over a 24-hour period.

The conclusions of this study are the following:

- The system proved to be sensitive to the EV penetration. Undervoltage was observed with only 8,05% of EV penetration in downstream buses of the system (sensitive buses). This is equivalent to 50,4 kW or 3 vehicles grouped in a block.
- The control technology implemented to mitigate undervoltage in the system is the V2G control, which does not require extra infrastructure installed by the distributor, since the outlets are already installed by EVs users. Among the results found, it is noted that the V2G control is an auxiliary control. Although the V2G does not act as main control to alleviate the undervoltage, it does improve the disturbances in the system. Also it proves to be attractive when compared to other forms of mitigation such as the installation of large battery banks that require large investments.
- The results show that the choice of the V2G control voltage reading point has a significant impact to mitigate system undervoltage. Control with reading at the PCC proved to be more assertive,

considering the buses located further downstream. On the other hand, voltage reading control on the secondary of medium to low voltage transformers was less assertive, indicates that a large part of the system prone to undervoltage is not adequately addressed from the control perspective. In fact, comparing the two types of reading, the reading at the PCC clearly proved to be more successful and advantageous in terms of implementation in real systems using V2G technology control.

- Also, the results indicate that the Droop curve chosen is conservative. In each case the V2G injects power into the system not only at times when there is undervoltage. The EV batteries deliver power to the grid for voltages equal and below 0,97 pu, modifying the voltage profile. This curve was strategically designed to prevent greater control oscillations, as the system showed this characteristic, generating power oscillations during V2G control. Therefore, other control strategies can be evaluated, such as intelligent control, as well as other Droop curves.
- As demonstrated in this work, the impact of undervoltage is intensified by the allocation of the EVs connected to the system buses. In other words, the location of the vehicle charging stations has a considerable impact on the level of undervoltage caused by the insertion of the vehicles. Therefore, if the sockets are installed in sensitive buses located downstream of the system, the impact is severe. One suggestion to distribution system operators is to encourage the location of public charging outlets for EVs on system buses that are less likely to cause technical disturbances.

Therefore, by using the EVs model and V2G proposed, this study can provide insights into the benefits, challenges and limitations of implementing V2G in real-world cases.

The authors would like to special thanks to Uppsala University, The Swedish Electromobily Center, Petrobras, Electrical Engineering Graduate Program and Federal University of Juiz de Fora, Coordination for the Improvement of Higher Education Personnel - CAPES, Fundação de Amparo à Pesquisa de Minas Gerais - FAPEMIG and INERGE.

The authors declare no conflict of interest.

References

References

Objetivos de Desenvolvimento Sustentável. (Access: 07 December, 2022).

Technology report Global EV Outlook 2022.. (Access: 08 December, 2022).

Nota Técnica nº 0076/2021-SRD/ANEEL. (June, 2021).

The potential impact of a mobility house on a congested distribution grid—a case study in Uppsala, Sweden. (2022). *CIREN Porto Workshop 2022: E-Mobility and Power Distribution Systems, 2022*, 1079–1083.

Potential of Load Shifting in a Parking Garage with Electric Vehicle Chargers, Local Energy Production and Storage. (2022). *World Electric Vehicle Journal*, 13(9), 166.

Otimização de carga e descarga de veículos elétricos considerando diferentes modelos tarifários. (2018). 97.

Adaptive control-based Isolated bi-directional converter for G2V& V2G charging with integration of the renewable energy source. (2022). *Energy Reports*, 8, 11416–11428.

Power converter topologies for grid-tied solar photovoltaic (PV) powered electric vehicles (EVs)—a comprehensive review. (2022). *Energies*, 15(13), 4648.

Privacy preservation for V2G networks in smart grid: A survey. (2016). *Computer Communications*, 91, 17–28.

- Assessing the EV Hosting Capacity of Australian Urban and Rural MV-LV Networks. (2022). *Electric Power Systems Research*, 212, 108399.
- How electric vehicles and the grid work together: Lessons learned from one of the largest electric vehicle trials in the world. (2018). *IEEE Power and Energy Magazine*, 16(6), 64–76.
- Statistical representation of EV charging: Real data analysis and applications. (2018). *2018 Power Systems Computation Conference (PSCC)*, 1–7.
- Análise dos impactos dos veículos elétricos nos sistemas de distribuição considerando o modo V2G e o transporte de energia.* (2020).
- Integrated PV Charging of EV Fleet Based on Energy Prices, V2G and Offer of Reserves. (2019). *IEEE Transactions on Smart Grid*, 10(2), 1313–1325.
- Nissan Leaf to stabilise the German electricity grid.* (Access: 7 February, 2023).
- V2G Redispatch - TenneT, Nissan, The Mobility House.* (Access: 17 February, 2023).
- Eletromobilidade no Brasil.* (Access: 12 December, 2022).
- Experimental validation of a battery dynamic model for EV applications.. (2009). *World Electric Vehicle Journal.*, 3(2), 289–298.
- Aplicação de modelos elétricos de bateria na predição do tempo de vida de dispositivos móveis.* (2012).
- Voltage-sourced converters in power systems: modeling, control, and applications.* (2010). John Wiley & Sons.
- Simplified electric vehicle powertrain model for range and energy consumption based on EPA coast-down parameters and test validation by Argonne National Lab data on the Nissan Leaf. (2014). *2014 IEEE Transportation Electrification Conference and Expo (ITEC)*, 1–6.
- V2G parking lot with PV rooftop for capacity enhancement of a distribution system. (2013). *IEEE Transactions on Sustainable Energy*, 5(1), 119–127.
- (2013). Universidade Federal de Juiz de Fora.
- Assessing the challenges and opportunities of electric mobility through the optimization of carsharing considering demand uncertainty.* (2022). 105.
- Ant colony optimization. (2006). *IEEE Computational Intelligence Magazine*, 1(4), 28–39.
- Ant colony optimization: overview and recent advances.* (2019). Springer.
- Technical and economic analysis of battery storage for residential solar photovoltaic systems in the Brazilian regulatory context. (2020). *Energies*, 13(24), 6517.
- Análise Econômica para Inclusão de Baterias de Segunda Vida para Prossumidores no Brasil. (2021). *Simpósio Brasileiro De Automação Inteligente-SBAI*, 1(1).
- Procedimentos de Distribuição de Energia Elétrica no Sistema Elétrico Nacional – PRODIST - Módulo 8.* (Access: 24 December, 2022).